

Dibenzylzirconium Complexes of Chelating Aminodiols. Synthesis, Structural Studies, Thermal Stability, and Insertion Chemistry

Pengcheng Shao,[†] Roland A. L. Gendron, David J. Berg,* and Gordon W. Bushnell

Department of Chemistry, University of Victoria, P.O. Box 3065, Victoria, British Columbia, Canada V8W 3V6

Received September 20, 1999

Aminodiolate ligands, $\text{RN}(\text{CH}_2\text{CH}_2\text{C}(\text{O})\text{R}')_2$ (**1a–e**), allow the isolation of soluble, monomeric zirconium dialkyl complexes, $[\text{RN}(\text{CH}_2\text{CH}_2\text{C}(\text{O})\text{R}')_2]\text{ZrR}''_2$ (**2a–e**, **5**, **6**). The fluxional behavior and thermal stability of these complexes are strongly dependent on the nature of the substituents at the nitrogen center, with smaller substituents ($\text{R} = \text{Me}$; **2a,b**, **5**, **6**) increasing the rigidity and thermal stability of the complexes. Complexes bearing *tert*-butyl groups (**2c,d**) readily undergo thermal decomposition by elimination of isobutene. Thermal ortho metalation of the chiral complex $\text{Zr}[\{(\text{S})\text{-PhC}(\text{H})\text{Me}\}\text{N}(\text{CH}_2\text{CH}_2\text{C}(\text{O})\text{Me}_2)[\text{CH}_2\text{Ph}]]_2$ (**2e**) affords the chiral metallacycle $\text{Zr}[\text{N}\{\text{CH}_2\text{CH}_2\text{C}(\text{O})\text{Me}_2\}_2\{(\text{S})\text{-2-C}_6\text{H}_4\text{C}(\text{H})\text{Me}\}][\text{CH}_2\text{Ph}]$ (**7**), which has been structurally characterized. Reaction of **7** with 1 equiv of aryl aldehyde ($\text{ArC}(\text{O})\text{H}$; $\text{Ar} = \text{Ph}$, β -naphthyl) results in regioselective insertion of the aldehyde into the phenyl–zirconium bond. The resulting aminotriolate complex $\text{Zr}[\text{N}\{\text{CH}_2\text{CH}_2\text{C}(\text{O})\text{Me}_2\}_2\{((\text{S})\text{-2-}((\text{R})\text{-}(\beta\text{-naphthyl})\text{CH}(\text{O}))\text{-C}_6\text{H}_4\text{C}(\text{H})\text{Me}))[\text{CH}_2\text{Ph}]]$ (**8b**) is formed in 91% de and has been characterized by X-ray crystallography. Further insertion of $\text{ArC}(\text{O})\text{H}$ into the remaining Zr–benzyl bond of **8b** proceeds with poorer stereochemical control. Complex **7** also catalyzes the slow cyclotrimerization of phenylacetylene to 1,2,4- and 1,3,5-triphenylbenzene (2.5 turnovers/day). Complexes **2b,d** and **7** function as precatalysts for ethylene polymerization when treated with MAO activator, although the activity is very low.

Introduction

The vast majority of early-transition-metal and f-element organometallic chemistry is supported by the cyclopentadienyl group, or its derivatives, as ancillary ligation.¹ While this class of ligands remains extremely productive, an ever-increasing number of researchers are turning their attention to alternative ligands.² Much of the motivation for this work is the belief that the dramatically different steric and electronic environments available with these supporting ligands will result in new and unusual reactivity for the metal–carbon bond not seen in cyclopentadienyl complexes. Simple monodentate and polydentate alkoxides have been used extensively in this role.³ Alkoxide-based group 4 organometallic compounds have been used as alkene polymerization⁴ and alkyne cyclotrimerization⁵ catalysts. Chelating alkoxide complexes, such as those derived from triethanolamine,⁶ have been prepared which display remarkable kinetic stability. Recently, chiral analogues of these complexes have been shown

to offer promising stereoselectivity in epoxide ring opening with azidotrialkylsilanes and in oxidation of alkyl aryl sulfides.⁷ Similarly, chiral binaphtholate (BINOL) complexes have been explored.⁸

In this contribution, we report the synthesis and reactivity of zirconium alkyl complexes containing a series of chelating aminodiolate ligands, derived from the aminodiols $\text{RN}(\text{CH}_2\text{CH}_2\text{C}(\text{OH})\text{R}')_2$ (**1a–e**). The aminodiolate framework is of interest for several rea-

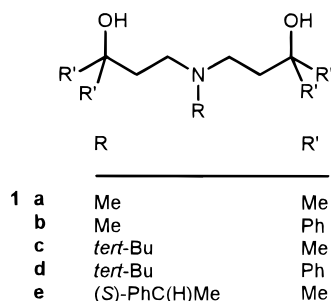
* To whom correspondence should be addressed.

[†] Current address: Department of Chemistry, University of Rochester, Rochester, NY 14620.

(1) (a) Marks, T. J.; Ernst, R. D. In *Comprehensive Organometallic Chemistry*; Wilkinson, G., Stone, F. G. A., Abel, E. W., Eds.; Pergamon: New York, 1982; Vol. 3, p 173. (b) Sikora, D. J.; Macomber, D. W.; Rausch, M. D. *Adv. Organomet. Chem.* **1986**, *25*, 317. (c) Schaverien, C. J. *Adv. Organomet. Chem.* **1994**, *36*, 283. (d) Jordan, R. *Adv. Organomet. Chem.* **1991**, *32*, 325. (e) Bochmann, M. *J. Chem. Soc., Dalton Trans.* **1996**, 255.

(2) See for example: (a) Floriani, C.; Ciurli, S.; Chiesi-Villa, A.; Guastini, C. *Angew. Chem., Int. Ed. Engl.* **1987**, *26*, 70. (b) Yang, C. H.; Ladd, J. A.; Goedken, V. L. *J. Coord. Chem.* **1988**, *18*, 317. (c) Cotton, F. A.; Czuchajowska, J. *Polyhedron* **1990**, *21*, 2553. (d) DeAngelis, S.; Solari, E.; Gallo, E.; Chiesi-Villa, A.; Floriani, C.; Rizzoli, C. *Inorg. Chem.* **1992**, *31*, 2520. (e) Uhrhammer, R.; Black, D. G.; Gardner, T. G.; Olsen, J. D.; Jordan, R. F. *J. Am. Chem. Soc.* **1993**, *115*, 8493. (f) Jacoby, D.; Floriani, C.; Chiesi-Villa, A.; Rizzoli, C. *J. Am. Chem. Soc.* **1993**, *115*, 3595. (g) Arnold, J.; Hoffman, C. G. *J. Am. Chem. Soc.* **1990**, *112*, 8620. (h) Schaverien, C. J. *J. Chem. Soc., Chem. Commun.* **1991**, 458. (i) Schaverien, C. J.; Orpen, A. G. *Inorg. Chem.* **1991**, *30*, 4968. (j) Shibata, K.; Aida, T.; Inoue, S. *Tetrahedron Lett.* **1992**, *33*, (k) Shibata, K.; Aida, T.; Inoue, S. *Chem. Lett.* **1992**, 1173. (l) Brand, H.; Arnold, J. *J. Am. Chem. Soc.* **1992**, *114*, 2266. (m) Brand, H.; Arnold, J. *Organometallics* **1993**, *12*, 3655. (n) Kim, H.-J.; Whang, D.; Kim, K.; Do, Y. *Inorg. Chem.* **1993**, *32*, 360. (o) Ryu, S.; Whang, D.; Kim, J.; Yeo, W.; Kim, K. *J. Chem. Soc., Dalton Trans.* **1993**, 2005. (p) Dell'Amico, G.; Marchetti, F.; Floriani, C. *J. Chem. Soc., Dalton Trans.* **1982**, 2197. (q) Mazzanti, M.; Rosset, J. M.; Floriani, C.; Chiesi-Villa, A.; Guastini, C. *J. Chem. Soc., Dalton Trans.* **1989**, 953. (r) Floriani, C. *Polyhedron* **1989**, *8*, 1717. (s) Cobrazza, F.; Solari, E.; Floriani, C.; Chiesi-Villa, A.; Guastini, C. *J. Chem. Soc., Dalton Trans.* **1990**, (t) Solari, E.; Floriani, C.; Chiesi-Villa, A.; Rizzoli, C. *J. Chem. Soc., Dalton Trans.* **1992**, 367. (u) Tjaden, E. B.; Swenson, D. C.; Jordan, R. F.; Petersen, J. L. *Organometallics* **1995**, *14*, 371.

(3) Rothwell, I. P. *Acc. Chem. Res.* **1988**, *21*, 153.



sons. The chelating nature of the ligand is expected to increase the stability of the complexes with respect to ligand redistribution. Additionally, the steric and electronic properties of the ligand can be tuned by varying the alkoxide carbon and amine nitrogen substituents. Incorporation of substituents at the alkoxide carbon is particularly desirable, because this helps to prevent formation of oligomeric species via alkoxide bridges.^{6,9} In the course of this work, it has become increasingly clear that the substituent at nitrogen is far from innocent and in fact plays a pivotal role in the thermal and coordinative stability of these complexes.

Experimental Section

General Procedures. All manipulations were carried out under an argon atmosphere, with the rigorous exclusion of oxygen and water, using standard glovebox (Braun MB150-GII) or Schlenk techniques. Tetrahydrofuran (THF), hexane, and toluene were dried by distillation from sodium benzophenone ketyl under argon immediately prior to use. Tetrabenzylzirconium¹⁰ and $\text{Zr}[\text{N}(\text{SiMe}_3)_2]_2\text{Cl}_2$ ¹¹ were prepared according to literature procedures. The synthesis of aminodiol ligands

1a–e and the bis(ligand) complexes $\text{Zr}[\text{RN}(\text{CH}_2\text{CH}_2\text{C}(\text{O})\text{R}')_2]_2$ (**3a–e**) is described elsewhere.¹²

¹H (360 MHz), ¹³C (90.55 MHz), ¹⁹F (338.86 MHz), and all variable-temperature NMR spectra were recorded on a Bruker AMX 360 MHz spectrometer. Spectra were recorded in *d*₆-benzene, *d*₈-toluene, or *d*₈-THF solvent, previously distilled from sodium under argon, using 5 mm tubes fitted with a Teflon valve (Brunfeldt) at room temperature unless otherwise specified. ¹H and ¹³C NMR spectra were referenced to residual solvent resonances. ¹⁹F NMR spectra were referenced to external CCl₃F. Proton and carbon NMR assignments were confirmed by ¹H–¹H or ¹H–¹³C COSY experiments for most compounds. Melting points were recorded using a Reichert hot stage and are not corrected. Elemental analyses were performed by Canadian Microanalytical, Delta, BC, Canada, or Atlantic Microanalytical, Atlanta, GA. Despite the use of co-oxidants such as V₂O₅ and PbO₂, the analytical data for most complexes were consistently 2–4% low in carbon. This may be due to metal carbide formation. Mass spectra were recorded on a Finnegan 3300 or a Kratos Concept H spectrometer using chemical ionization, electron impact (70 eV), or positive ion liquid secondary ionization (+LSIMS) methods.

Zirconium Dialkyl Complexes. The zirconium dialkyl complexes **2a–e**, **5**, and **6** were prepared by hydrocarbon elimination (**2a–e**), ligand redistribution (**2c–e**), or metathesis (**2b**, **5**, and **6**). Representative examples of each procedure are given as follows, followed by characterization data for each new complex.

(a) Hydrocarbon Elimination. A solution of **1d** (0.829 g, 1.68 mmol) in 10 mL of toluene was added dropwise to a stirred solution of tetrabenzylzirconium (0.763 g, 1.68 mmol) in 10 mL of toluene. After the mixture was stirred for 30 min, the solvent was removed in vacuo to afford **2d** as an off-white powder. Recrystallization from a toluene–hexane mixture afforded pale yellow crystals.

(b) Ligand Redistribution. A solution of **3d** (1.08 g, 1.00 mmol) in 20 mL of toluene was added to solid tetrabenzylzirconium (0.456 g, 1.00 mmol). The solution was stirred for 30 min, and the solvent was removed to yield **2d** as a powder. Recrystallization as above yielded pale yellow needles.

(c) Metathesis. A solution of (trimethylsilyl)lithium (0.061 g, 0.66 mmol) in toluene (20 mL) was added to a suspension of **4** (0.20 g, 0.33 mmol), prepared as described below, in 20 mL of toluene. The solution increased in cloudiness immediately on addition of the lithium reagent but slowly decreased in turbidity overnight. The solution was filtered through a Celite plug on a glass frit, and the resulting clear yellow filtrate was evaporated to yield a sticky yellow-brown oil which solidified on standing. The solid was recrystallized from hexane at –30 °C to afford yellow crystalline **5**.

Zr[MeN(CH₂CH₂C(O)Me)₂][CH₂Ph]₂ (2a**).** Yellow oil. The product contained significant amounts of tetrabenzylzirconium (identified by the characteristic doublet in the ¹H NMR at 6.39 ppm) and **3a** (ca. 20%), which could not be removed. Yield: 56%. ¹H NMR (*d*₆-benzene): δ 7.0–7.2 (m, 9H, aryl *H*), 6.72 (tt, 1H, *p*-benzyl *H*, ³*J*_{HH} = 7.1 Hz, ⁴*J*_{HH} = 1.4 Hz), 2.56 (s, 2H, ZrCH₂), 2.49 (t, 2H, NCH₂CH₂, *J*_{HH} = 13.2 Hz), 1.64 (s, 2H, ZrCH₂), 1.26 (m, 2H, NCH₂CH₂), 1.25 (s, 6H, C(O)Me_a), 1.24 (s, 3H, MeN), 1.22 (s, 6H, C(O)Me_b), 1.03 (m, 2H, NCH₂CH₂). ¹³C{¹H} NMR (*d*₆-benzene): δ 150.1, 137.9 (quat aryl C); 130.3, 129.7, 129.3, 128.6 (*o,m* aryl C); 122.8, 120.3 (*p* aryl C); 73.2 (ZrOC); 58.0 (NCH₂); 53.4, 52.7 (ZrCH₂, ¹*J*_{CH} = 130 Hz); 38.7 (CH₂C(O)); 37.7 (MeN); 32.7, 30.3 (C(O)Me).

(4) (a) Fandos, R.; Meetsma, A.; Teuben, J. H. *Organometallics* **1991**, 10, 59. (b) Fandos, R.; Teuben, J. H.; Helgesson, G.; Jagner, S. *Organometallics* **1991**, 10, 1637. (c) Rieger, B. J. *Organomet. Chem.* **1991**, 420, C17. (d) Masi, F.; Malguori, S.; Barazzoni, L.; Ferrero, C.; Moalli, A.; Marconi, F.; Invernizzi, R.; Zandora, N.; Altomare, A.; Ciardelli, F. *Makromol. Chem. Suppl.* **1989**, 15, 147. (e) Kakugo, M.; Miyatake, T.; Mizunuma, K. *Chem. Express* **1987**, 2, 445. (f) Miyatake, T.; Mizunuma, K.; Seki, Y.; Kakugo, M. *Makromol. Chem., Rapid Commun.* **1989**, 10, 349. (g) Miyatake, T.; Mizunuma, K.; Kakugo, M. *Makromol. Chem., Macromol. Symp.* **1993**, 66, 203. (h) Fokken, S.; Spaniol, T. P.; Kang, H. C.; Massa, W.; Okuda, J. *Organometallics* **1996**, 15, 5069. (i) Porri, L.; Ripa, A.; Colombo, P.; Moana, E.; Capelli, S.; Meille, S. V. *J. Organomet. Chem.* **1996**, 514, 213. (j) Fokken, S.; Spaniol, T. P.; Okuda, J.; Sernetz, F. G.; Mülhaupt, R. *Organometallics* **1997**, 16, 4240. (k) Floriani, C.; Corazza, F.; Lesueur, W.; Chiesi-Villa, A.; Guastini, C. *Angew. Chem., Int. Ed. Engl.* **1989**, 28, 66. (l) Corazza, F.; Floriani, C.; Chiesi-Villa, A.; Guastini, C. *Inorg. Chem.* **1991**, 30, 146. (m) Okuda, J.; Fokken, S.; Kang, H. C.; Massa, W. *Chem. Ber.* **1995**, 128, 221.

(5) (a) van der Linden, A.; Schaverien, C. J.; Meijboom, N.; Ganter, C.; Orpen, A. G. *J. Am. Chem. Soc.* **1995**, 117, 3008. (b) Hill, J. E.; Fanwick, P. E.; Rothwell, I. P. *Organometallics* **1990**, 9, 2211. (c) Hill, J. E.; Balaich, G.; Fanwick, P. E.; Rothwell, I. P. *Organometallics* **1993**, 12, 2911.

(6) (a) Naiini, A. A.; Ringrose, S. L.; Su, Y.; Jacobson, R. A.; Verkade, J. G. *Inorg. Chem.* **1993**, 32, 1290. (b) Menge, W.; Verkade, J. G. *Inorg. Chem.* **1991**, 30, 4628. (c) Naiini, A.; Menge, W. M. P. B.; Verkade, J. G. *Inorg. Chem.* **1991**, 30, 5009.

(7) (a) Nugent, W. A.; Harlow, R. L. *J. Am. Chem. Soc.* **1994**, 116, 6142. (b) Bonchio, M.; Calloni, S.; DiFuria, F.; Licini, G.; Modena, G.; Moro, S.; Nugent, W. A. *J. Am. Chem. Soc.* **1997**, 119, 6935. (c) DiFuria, F.; Licini, G.; Modena, G.; Motterle, R.; Nugent, W. A. *J. Org. Chem.* **1996**, 61, 5175.

(8) (a) Boyle, T. J.; Barnes, D. L.; Heppert, J. A.; Morales, L.; Takusagawa, F.; Connolly, J. W. *Organometallics* **1992**, 11, 1112. (b) Boyle, T. J.; Eilerts, N. W.; Heppert, J. A.; Takusagawa, F. *Organometallics* **1994**, 13, 2218.

(9) Bradley, D. C.; Mehrotra, R. C.; Gaur, D. P. *Metal Alkoxides*; Academic Press: London, 1978.

(10) Zucchini, U.; Albizzati, E.; Giannini, U. *J. Organomet. Chem.* **1971**, 26, 357.

(11) Andersen, R. A. *J. Chem. Soc., Dalton Trans.* **1980**, 2010.

(12) The aminodiol ligands **1a–e** were prepared in two steps. Michael addition of the appropriate amine (RNH₂, 2 equiv) to methyl acrylate afforded the aminodiester RN(CH₂CH₂C(O)OMe)₂. The aminodiester were then converted to the aminodiol by reaction with 4 equiv of R'Li, followed by hydrolysis and standard workup. The bis(ligand) complexes **3a–e** were prepared from tetrabenzylzirconium¹⁰ and 2 equiv of the aminodiol **1a–e**. Full experimental details for these reactions will be reported elsewhere: Shao, P.; Gendron, R. A. L.; Berg, D. J. *Can. J. Chem.*, in press.

Zr[MeN(CH₂CH₂C(O)Ph)₂][CH₂Ph]₂ (2b). White crystals. Yield: 85%. Mp: 166–168 °C. ¹H NMR (*d*₆-benzene): δ 7.62 (d, 4H, *o* aryl *H*, *J*_{HH} = 7.4 Hz), 7.52 (d, 4H, *o* aryl *H*, *J*_{HH} = 7.6 Hz), 7.31 (t, 4H, aryl *H*, *J*_{HH} = 6.5 Hz), 6.9–7.2 (m, 17H, aryl *H*), 6.77 (t, 1H, aryl *H*, *J*_{HH} = 5.8 Hz), 2.58 (t, 2H, NCH₂CH₂, *J*_{HH} = 11.4 Hz), 2.34 (dd, 2H, NCH₂CH₂), 2.27 (s, 2H, ZrCH₂), 2.20 (t, 2H, NCH₂CH₂), 1.95 (s, 2H, ZrCH₂), 1.48 (dd, 2H, NCH₂CH₂, *J*_{HH} = 11.1, 5.7 Hz), 1.32 (s, 3H, MeN). ¹³C{¹H} NMR (*d*₆-benzene): δ 151.5, 148.4, 148.6, 139.2 (quat aryl C); 130.1, 130.0, 129.3, 128.6, 128.5, 128.4, 127.0, 126.8, 126.6, 125.3, 123.7, 121.3 (aryl C); 82.2 (ZrOC); 58.0 (NCH₂); 57.5, 55.4 (ZrCH₂, ¹*J*_{CH} = 130 Hz); 39.5 (MeN); 36.9 (CH₂C(O)). Anal. Calcd for C₄₅H₄₅NO₂Zr: C, 74.75; H, 6.27; N, 1.94. Found: C, 70.62; H, 6.11; N, 1.93.

Zr[*tert*-BuN(CH₂CH₂C(O)Me)₂][CH₂Ph]₂ (2c). Pale yellow oil. Yield: 95%. ¹H NMR (*d*₆-benzene): δ 7.09 (t, 4H, *m* benzyl *H*, *J*_{HH} = 5.8 Hz), 6.89 (t, 2H, *p* benzyl *H*, *J*_{HH} = 7.3 Hz), 6.79 (d, 4H, *o* benzyl *H*, *J*_{HH} = 8.2 Hz), 2.77 (m, 4H, NCH₂), 1.83 (s, 4H, ZrCH₂), 1.62 (m, 4H, CH₂C(O)), 1.06 (s, 12H, C(O)Me), 1.05 (s, 9H, *tert*-BuN). ¹H NMR (*d*₈-toluene, –60 °C): δ 7.03 (t, 4H, *m* benzyl *H*), 6.93 (t, 2H, *p* benzyl *H*), 6.80 (d, 4H, *o* benzyl *H*), 2.90 (br s, 2H, NCH₂), 2.72 (br s, 2H, NCH₂), 1.82 (s, 4H, ZrCH₂), 1.75 (br s, 2H, CH₂C(O)), 1.56 (br s, 2H, CH₂C(O)), 1.19 (s, 6H, C(O)Me), 1.08 (s, 9H, *tert*-BuN), 0.99 (s, 6H, C(O)Me). ¹³C{¹H} NMR (*d*₆-benzene): δ 144.0 (quat aryl C), 130.8 (*o* aryl C), 126.7 (*m* aryl C), 122.6 (*p* aryl C), 80.5 (ZrOC), 54.0 (Me₃CN), 52.9 (NCH₂), 43.2 (ZrCH₂, ¹*J*_{CH} = 128 Hz), 41.6 (CH₂C(O)), 30.3 (C(O)Me), 28.9 (Me₃CN).

Zr[*tert*-BuN(CH₂CH₂C(O)Ph)₂][CH₂Ph]₂ (2d). White microcrystalline powder. Yield: 90%. Mp: 180 °C dec. ¹H NMR (*d*₆-benzene): δ 7.35 (d, 8H, *o* phenyl *H*, *J*_{HH} = 7.4 Hz), 7.15 (t, 8H, *m* phenyl *H*, *J*_{HH} = 7.4 Hz), 7.04 (t, 4H, *m* benzyl *H*, *J*_{HH} = 8.5 Hz), 7.03 (d, 4H, *p* phenyl *H*, *J*_{HH} = 7.5 Hz), 6.90 (t, 2H, *p* benzyl *H*, *J*_{HH} = 7.3 Hz), 6.55 (d, 4H, *o* benzyl *H*, *J*_{HH} = 7.6 Hz), 2.69 (br t, 4H, NCH₂), 2.55 (t, 4H, CH₂C(O), *J*_{HH} = 6.4 Hz), 1.85 (s, 4H, ZrCH₂), 0.86 (s, 9H, *tert*-BuN); ¹³C{¹H} NMR (*d*₆-benzene): δ 148.2 (quat phenyl C); 143.6 (quat benzyl C); 128.5, 128.3, 127.9, 127.3, 126.9, 123.1 (aryl C); 87.3 (ZrOC); 59.0 (Me₃CN); 55.8 (br, NCH₂); 45.0 (br, CH₂C(O)); 41.1 (ZrCH₂, ¹*J*_{CH} = 129 Hz); 28.6 (Me₃CN). Anal. Calcd for C₄₈H₅₁NO₂Zr: C, 75.35; H, 6.72; N, 1.83. Found: C, 73.02; H, 6.76; N, 1.85. The ortho benzyl proton signal shifts to 6.70 ppm on addition of 0.1 mL of *d*₈-THF.

Zr[N(CH₂CH₂C(O)Me)₂]{*S*-PhC(H)Me}[CH₂Ph]₂ (2e). Colorless oil. Yield: 85%. ¹H NMR (*d*₆-benzene): δ 6.7–7.3 (m, 15H, aryl *H*), 3.96 (q, 1H, MeC(H)N, ³*J*_{HH} = 7.0 Hz), 2.75 (m, 2H, NCH₂), 2.29 (d, 2H, ZrCH₂, ²*J*_{HH} = 9.6 Hz), 2.13 (d, 2H, ZrCH₂, ²*J*_{HH} = 9.6 Hz), 1.95 (m, 2H, NCH₂), 1.65 (m, 2H, CH₂C(O)), 1.30 (m, 2H, CH₂C(O)), 1.26 (s, 6H, C(O)Me), 1.25 (d, 3H, MeC(H)N, ³*J*_{HH} = 7.0 Hz), 1.19 (s, 6H, C(O)Me). ¹³C{¹H} NMR (*d*₆-benzene): δ 146.2 (quat phenyl C); 141.1 (quat benzyl C); 129.3, 129.0, 128.8, 128.6, 128.2, 127.6 (aryl C); 75.5 (ZrOC); 58.7 (MeC(H)N); 58.6 (ZrCH₂, ¹*J*_{CH} = 126 Hz); 50.1 (NCH₂); 40.1 (CH₂C(O)); 31.7, 30.3 (C(O)Me); 21.7 (MeC(H)N). The complex slowly decomposes at room temperature by ortho metalation.

{Zr[MeN(CH₂CH₂C(O)Ph)₂][Cl]₂]_x (4). A solution of **1b** (2.00 g, 4.42 mmol) in 10 mL of toluene was added to a solution of Zr[N(SiMe₃)₂Cl]₂ (2.13 g, 4.42 mmol) in 30 mL of toluene. The reaction mixture was heated at 70 °C for 1 h, resulting in the precipitation of a large amount of white solid. The solid was isolated by filtration on a glass frit and washed repeatedly with toluene (100 mL total volume). The solid was dried under vacuum for several hours to yield a free-flowing white powder. Yield: 57%. Mp: 255–257 °C. ¹H NMR (*d*₅-pyridine; 107 °C): δ 7.9 (br s, 8H, aryl *H*), 7.25 (br s, 12H, aryl *H*), 2.6–3.3 (br unresolved singlet, 11H, backbone CH₂ and NMe). ¹³C{¹H} NMR (*d*₅-pyridine; 93 °C): δ 128.2, 129.0, 129.2 (aryl C), 56.8 (s, NCH₂), 37.7 (very broad singlet, CH₂C(O)). The methyl, ipso aryl, and alkoxide carbon resonances were not observed. Anal.

Calcd for C₃₁H₃₁NO₂ZrCl₂: C, 60.86; H, 5.11; N, 2.29. Found: C, 59.02; H, 5.15; N, 2.13.

Zr[MeN(CH₂CH₂C(O)Ph)₂][CH₂SiMe₃]₂ (5). Yellow crystals. Yield: 74%. Mp: 157–159 °C. ¹H NMR (*d*₆-benzene): δ 7.73 (d, 4H, *o* aryl *H*, *J*_{HH} = 7.2 Hz), 7.48 (d, 4H, *o* aryl *H*, *J*_{HH} = 7.2 Hz), 7.25 (t, 4H, *m* aryl *H*, *J*_{HH} = 7.8 Hz), 7.15 (t, 4H, *m* aryl *H*, *J*_{HH} = 7.8 Hz), 7.06 (t, 2H, *p* aryl *H*, *J*_{HH} = 7.3 Hz), 7.00 (t, 2H, *p* aryl *H*, *J*_{HH} = 7.4 Hz), 2.20 (m, 6H, NCH_{2a,b} and CH_{2a}C(O) overlapping), 1.62 (s, 3H, MeN), 1.58 (m, 2H, CH_{2b}C(O)), 0.84 (s, 2H, ZrCH_{2a}), 0.69 (s, 2H, ZrCH_{2b}), 0.33 (s, 9H, SiMe_{3a}), 0.23 (s, 9H, SiMe_{3b}). ¹³C{¹H} NMR (*d*₆-benzene): δ 149.7, 148.1 (quat aryl C); 128.4, 126.8, 126.5, 126.0 (aryl C); 83.6 (ZrOC); 57.6 (NCH₂); 52.4 (ZrCH_{2a}); 51.8 (ZrCH_{2b}); 42.2 (MeN); 37.9 (CH₂C(O)); 3.4 (SiMe_{3a}); 3.2 (SiMe_{3b}). Anal. Calcd for C₃₉H₅₃NO₂Si₂Zr: C, 65.49; H, 7.47; N, 1.96. Found: C, 63.04; H, 6.01; N, 2.27. MS (EI): *m/z* 698 (M⁺ – Me, 3%), 626 (M⁺ – CH₂SiMe₃, 50%), 180 (100%). Simulation of the M⁺ – CH₂SiMe₃ envelope: *m/z*, obsd intensity (calcd intensity) 626, 100% (100); 627, 62% (60); 628, 57% (53); 629, 20% (19); 630, 36% (37); 631, 14% (13); 632, 10% (5); 633, 4% (2).

Zr[MeN(CH₂CH₂C(O)Ph)₂][Me]₂ (6). Dark brown oil. Yield: ca. 40%. ¹H NMR (*d*₆-benzene): δ 7.85 (d, 4H, *o* aryl *H*, *J*_{HH} = 7.3 Hz), 7.69 (d, *o* aryl *H*, *J*_{HH} = 7.3 Hz), 7.27 (t, 4H, *m* aryl *H*, *J*_{HH} = 7.8 Hz), 7.05–7.20 (m, 6H, *m,p* aryl *H*), 6.99 (t, 2H, *p* aryl *H*, *J*_{HH} = 7.3 Hz), 2.25 (m, 6H, NCH_{2a,b} and CH_{2a}C(O) overlapping), 1.48 (m, 2H, CH_{2b}C(O)), 1.43 (s, 3H, MeN), 0.84 (s, 3H, ZrMe_a), 0.75 (s, 3H, ZrMe_b); ¹³C{¹H} NMR (*d*₆-benzene): δ 150.8, 148.4 (quat aryl C); 128.4, 128.3, 126.7, 126.6, 126.5, 125.4 (aryl C); 82.3 (ZrOC); 57.4 (NCH₂); 38.5 (MeN); 37.9 (CH₂C(O)); 37.6 (ZrMe_a); 34.8 (ZrMe_b).

Thermal Decomposition Studies. The decomposition of **2a–e** was followed by NMR spectroscopy. In each experiment, 30 mg of complex was dissolved in 0.8 mL of *d*₈-toluene and the sample placed in a hot oil bath. The ¹H spectrum of the complex was monitored periodically. Kinetic studies were carried out in a similar fashion, except that the sample was heated in the NMR probe and the amount of starting complex remaining and product formed (in the case of **7**) were established by integration. Preparative scale experiments were carried out by heating 0.5–1.0 g of the appropriate dialkyl in an oil bath for a period of time previously established as sufficient to complete the conversion.

Zr[N(CH₂CH₂C(O)Me)₂]{*S*-2-C₆H₄C(H)Me}[CH₂Ph] (7). Pale yellow crystals. Yield: 60%. Mp: 175 °C. ¹H NMR (*d*₆-benzene): δ 8.16 (m, 1H, α phenyl *H*), 7.35 (m, 1H, *o* benzyl *H*), 7.30 (m, 2H, β,γ phenyl *H*), 7.25 (m, 1H, *m* benzyl *H*), 7.03 (m, 1H, δ phenyl *H*), 6.90 (tt, *p* benzyl *H*, *J*_{HH} = 7.3, 1.2 Hz), 4.61 (q, 1H, MeC(H)N, ³*J*_{HH} = 6.9 Hz), 3.10 (d, 1H, ZrCH_{2a}, ²*J*_{HH} = 9.1 Hz), 3.00 (d, 1H, ZrCH_{2b}, ²*J*_{HH} = 9.1 Hz), 2.81 (m, 1H, NCH_{2a}), 2.71 (m, 1H, NCH_{2b}), 1.80 (m, 2H, NCH_{2c,d}), 1.78 (m, 1H, CH_{2a}C(O)), 1.58 (m, 1H, CH_{2b}C(O)), 1.04 (s, 3H, C(O)Me_a), 1.03 (s, 3H, C(O)Me_b), 1.02 (m, 1H, CH_{2c}C(O)), 0.96 (s, 3H, C(O)Me_c), 0.92 (m, 1H, CH_{2d}C(O)), 0.89 (d, 3H, MeC(H)N, ³*J*_{HH} = 6.9 Hz), 0.83 (s, 3H, C(O)Me_d). The designators α–γ refer to the position with respect to the metalated phenyl ring carbon, with α being adjacent to this site. ¹³C{¹H} NMR (*d*₆-benzene): δ 182.9 (phenyl C–Zr); 152.2 (quat phenyl C); 144.1 (quat benzyl C); 139.4, 129.8, 128.9, 127.6, 125.8, 123.5, 121.5 (aryl C); 76.2 (ZrOC_a); 74.8 (ZrOC_b); 60.5 (ZrCH₂, ¹*J*_{CH} = 131 Hz); 59.5 (MeC(H)N); 46.9 (NC_aH₂); 46.7 (NC_bH₂); 37.9 (C_aH₂C(O)); 37.6 (C_bH₂C(O)); 32.5, 31.6, 30.3, 30.2 (C(O)Me); 7.6 (MeC(H)N). MS (EI): *m/z* 471 (M⁺, 5%), 380 (M⁺ – CH₂Ph, 15%), 91 (C₇H₇⁺, 100%). Anal. Calcd for C₂₅H₃₅NO₂Zr: C, 63.51; H, 7.46; N, 2.96. Found: C, 61.49; H, 7.26; N, 2.97.

Insertion Reactions. (i) Phenyl–Zr Insertion. A solution of benzaldehyde or β-naphthaldehyde in toluene (0.25 mmol in 10 mL) was rapidly added to a cooled (–30 °C) toluene solution of **7** (0.25 mmol in 20 mL). The reaction mixture was stirred for 1 h while still cold and then warmed to room temperature. Removal of solvent in vacuo afforded the insertion product as a white or yellow powder. In some experiments

the solid product was hydrolyzed at this stage to release the organic ligand and the diastereomeric excess was determined by ^1H NMR integration of unique resonances (detailed below). In other experiments, the solid complex was recrystallized from a toluene–hexane mixture and the NMR recorded.

(ii) Benzyl–Zr Insertion. A solution of benzaldehyde or β -naphthaldehyde in toluene (0.5 mmol in 10 mL) was added to a cooled (-30°C) toluene solution of **7** (0.25 mmol in 20 mL), and the reaction mixture was warmed to room temperature with stirring. After 6 h, the solution was quenched with 2 mL of H_2O and the organic product was extracted in Et_2O . The Et_2O phase was dried over MgSO_4 , and the product was isolated as a pale yellow oil after removal of the solvent. The enantiomeric excess of the benzyl insertion product was determined by GC on a β -Dex column and by NMR using europium tris[3-(trifluoromethylhydroxymethylene)-(+)-camphorate] as a chiral shift reagent.

Zr[N(CH₂CH₂C(O)Me)₂]{(S)-2-((R)-PhCH(OH))-C₆H₄C(H)Me}[CH₂Ph] (8a). Pale yellow crystals. Yield: 55%. Mp: 179–183 $^\circ\text{C}$. The ^1H and ^{13}C NMR spectra of this complex are extremely broad and are poorly resolved at all temperatures. Anal. Calcd for $\text{C}_{32}\text{H}_{41}\text{NO}_3\text{Zr}$: C, 66.39; H, 7.14; N, 2.42. Found: C, 61.59; H, 6.78; N, 2.37. The poor analytical data and inability to obtain meaningful NMR data render the identification of this compound tentative.

Zr[N(CH₂CH₂C(O)Me)₂]{(S)-2-((R)-(β -naphthyl)CH(OH))-C₆H₄C(H)Me}[CH₂Ph] (8b). Pale yellow crystals. Yield: 71%. Mp: 155–156 $^\circ\text{C}$. ^1H NMR (d_6 -benzene, 50°C): δ 6.9–7.8 (m, 16H, aryl *H*), 6.10 (s, 1H, C(*H*)OZr), 4.51 (q, 1H, MeC(*H*)N, $^3J_{\text{HH}} = 7.0$ Hz), 3.02 (br m, 1H, CH₂), 2.84 (br m, 1H, CH₂), 2.69 (d, 1H, ZrCH₂, $^2J_{\text{HH}} = 10.2$ Hz), 2.66 (d, 1H, ZrCH₂, $^2J_{\text{HH}} = 10.2$ Hz), 1.90 (m, 1H, CH₂), 1.80 (m, 1H, CH₂), 1.60 (m, 1H, CH₂), 1.45 (m, 1H, CH₂), 1.38 (s, 3H, C(O)Me_a), 1.09 (s, 6H, C(O)Me_{b,d}), 1.00 (m, 2H, CH₂), 0.65 (s, 3H, C(O)Me_d), 0.60 (d, 3H, MeC(H)N, $^3J_{\text{HH}} = 7.0$ Hz). $^{13}\text{C}\{^1\text{H}\}$ NMR (d_6 -benzene, 50°C): δ 150.4, 145.9, 143.9, 139.3, 133.7, 132.9, 132.5, 130.6, 128.3, 127.3, 127.2, 126.2, 125.8, 124.3, 123.7, 119.7 (aryl *C*); 83.8 (ZrOC(H)); 76.1, 75.5 (ZrOCMe); 54.4 (ZrCH₂); 54.3 (MeC(H)N); 47.1, 46.9 (NCH₂); 40.6, 38.2 (CH₂C(O)); 32.7, 28.5 (br, C(O)Me); 11.4 (MeC(H)N). Anal. Calcd for $\text{C}_{36}\text{H}_{43}\text{NO}_3\text{Zr}$: C, 68.75; H, 6.89; N, 2.23. Found: C, 66.39; H, 6.79; N, 1.81.

N(CH₂CH₂C(OH)Me)₂]{(S)-2-((R)- and (S)-PhCH(OH))-C₆H₄C(H)Me} (9a). *SS:SR* ratio: 1:13 (93% de). ^1H NMR (CDCl_3): *SR* (major) δ 7.1–7.3 (m, 9H, aryl *H*), 5.77 (s, 1H, PhCH(OH)), 3.89 (q, 1H, MeC(H)N, $^3J_{\text{HH}} = 7.0$ Hz), 2.68 (m, 2H, NCH_{2a}), 2.40 (m, 2H, NCH_{2b}), 1.60 (m, 2H, CH_{2a}C(O)), 1.40 (m, 2H, CH_{2b}C(O)), 1.16 (d, 3H, MeC(H)N, $^3J_{\text{HH}} = 7.0$ Hz), 1.07 (s, 6H, C(O)Me_a), 1.06 (s, 6H, C(O)Me_b); *SS* (minor) δ 6.15 (s, 1H, PhCH(OH)), 4.57 (q, 1H, MeC(H)N). The remaining protons overlap with those of the major diastereomer. High-resolution MS (+LSIMS, *m*-nitrobenzoic acid): *m/z* found (calcd) $\text{M}^+ + \text{H}$ 400.2859 (400.2851).

N(CH₂CH₂C(OH)Me)₂]{(S)-2-((R)- and (S)- β -naphthyl)-CH(OH))-C₆H₄C(H)Me} (9b). *SS:SR* ratio: 1:10 (91% de). ^1H NMR (CDCl_3): *SR* (major) δ 7.1–7.9 (m, 11H, aryl *H*), 5.92 (s, 1H, ArC(OH)*H*), 3.94 (q, 1H, MeC(H)N, $^3J_{\text{HH}} = 6.8$ Hz), 2.70 (m, 2H, NCH_{2a}), 2.40 (m, 2H, NCH_{2b}), 1.62 (m, 2H, CH_{2a}C(O)), 1.42 (m, 2H, CH_{2b}C(O)), 1.10 (d, 3H, MeC(H)N, $^3J_{\text{HH}} = 7.0$ Hz), 1.08 (s, 12H, C(O)Me_{ab}); *SS* (minor) δ 6.33 (s, 1H, ArCH(OH)), 4.68 (q, 1H, MeC(H)N). The remaining protons overlap with those of the major diastereomer. High-resolution MS (+LSIMS, *m*-nitrobenzoic acid): *m/z* found (calcd) $\text{M}^+ + \text{H}$ 450.3002 (450.3007).

PhC(OH)(H)(CH₂Ph) (10a). ^1H NMR (CDCl_3): δ 7.15–7.35 (m, 10H, aryl *H*), 4.90 (dd, 1H, PhC(OH)*H*, $^3J_{\text{HH}} = 12.4$, 4.9 Hz), 3.02 (m, 2H, C(OH)CH_{2a}). $^{13}\text{C}\{^1\text{H}\}$ NMR (CDCl_3): δ 143.8, 138.0 (quat aryl *C*); 138.0, 129.5, 128.5, 128.4, 127.6, 127.6, 125.9 (*o,m,p* aryl *C*); 75.3 (C(OH)); 46.1 (CH₂). This product was identical with an authentic sample prepared from

benzyl lithium and benzaldehyde. High-resolution MS (EI): *m/z* found (calcd) $\text{M}^+ 198.1046$ (198.1045).

(β -naphthyl)C(OH)(H)(CH₂Ph) (10b). ^1H NMR (CDCl_3): δ 8.52 (s, 1H, α naphthyl *H*), 7.2–8.1 (m, 11H, aryl *H*), 5.08 (m, 1H, C(OH)*H*), 3.09 (m, 2H, C(OH)CH_{2a,b}). MS (EI): *m/z* 248 (M^+ , 20%), 247 ($\text{M}^+ - \text{H}$, 100%), 231 ($\text{M}^+ - \text{OH}$, 25%). High-resolution MS (EI): *m/z* found (calcd) $\text{M}^+ 248.1199$ (248.1201).

Zirconium Alkyl Cations. Treatment of a toluene (5 mL) solution of **2b** or **2e** (0.1 mmol) with 1 equiv of $\text{B}(\text{C}_6\text{F}_5)_3$ resulted in immediate formation of a yellow-orange oil which separated from solution. The toluene supernatant was decanted, and the oil was washed with 3×100 mL of hexane. Vacuum drying afforded the cations as semisolids which generated viscous orange oils on exposure to traces of toluene.

Zr[MeN(CH₂CH₂C(O)Ph)₂][CH₂Ph]⁺[B(C₆F₅)₃(CH₂Ph)][−] (11a). ^1H NMR (d_6 -benzene): δ 6.7–7.3 (br m, 30H, aryl *H*), 6.05 (br d, 2H, *o* benzyl *H*), 3.42 (br s, 2H, BCH₂), 1.3–3.2 (br m, 13H, ligand backbone and ZrCH₂). $^{19}\text{F}\{^1\text{H}\}$ NMR (d_6 -benzene): δ 166.9, 166.5, 165.3, 165.2, 164.7, 164.6, 163.4, 162.8, 161.3, 161.2, 160.6, 160.5, 160.4 (*m,p* aryl *F*); 130.9, 130.8, 130.4, 130.3 (*o* aryl *F*). $^{19}\text{F}\{^1\text{H}\}$ NMR (5:1 d_6 -benzene– d_8 -THF): δ −166.9 (t, 6F, *m* aryl *F*, $^3J_{\text{FF}} = 20$ Hz), −164.1 (t, 3F, *p* aryl *F*, $^3J_{\text{FF}} = 20$ Hz), −130.6 (d, 6F, *o* aryl *F*, $^3J_{\text{FF}} = 20$ Hz). $^{13}\text{C}\{^1\text{H}\}$ NMR (d_5 -bromobenzene): δ 148.9, 148.0, 147.6, 145.1, 142.6 (ipso aryl *C*); 148.9 (d, $^1J_{\text{CF}} = 224$ Hz, aryl CF), 148.0 (m, ipso aryl CF), 137.8 (d, $^1J_{\text{CF}} = 243$ Hz, aryl CF), 136.8 (d, $^1J_{\text{CF}} = 242$ Hz, aryl CF); 129.3, 129.3, 128.8, 128.6, 128.5, 127.9, 127.8, 127.4, 127.0, 126.9, 126.4, 126.3, 125.9, 125.6, 123.1, 122.8, 122.1 (aryl CH); 87.5, 85.1 (C(O)Me₂); 56.5 (ZrCH₂); 38.3, 37.3, 37.0, 36.3, 30.2 (CH₂ and NMe); 32.0 (br s, BCH₂). $^{19}\text{F}\{^1\text{H}\}$ NMR (d_5 -bromobenzene): δ −165.9 (t), −163.0 (t), −129.9 (d).

Zr[N(CH₂CH₂C(O)Me)₂]{(S)-2-C₆H₄C(H)Me}[CH₂Ph]⁺[B(C₆F₅)₃(CH₂Ph)][−] (11b). ^1H NMR (5:1 d_6 -benzene– d_8 -THF): δ 6.95–7.15 (m, 8H, aryl *H*), 6.83 (t, 1H, *p* benzyl *H*, $J_{\text{HH}} = 6.7$ Hz), 4.54 (br m, 1H, MeC(H)N), 3.37 (br s, 2H, BCH₂), 2.84 (br t, 1H, NCH_{2a}, $J_{\text{HH}} = 9.7$ Hz), 2.57 (t, 1H, NCH_{2b}, $J_{\text{HH}} = 13.4$ Hz), 2.14 (br m, 1H, NCH_{2d}), 1.94 (br m, 1H, NCH_{2d}), 1.88 (t, 1H, CH_{2a}C(O), $J_{\text{HH}} = 13.4$ Hz), 1.68 (t, 1H, CH_{2b}C(O), $J_{\text{HH}} = 14.2$ Hz), 1.33 (m, 1H, CH_{2c}(O)), 1.10 (CH_{2c}(O)), 1.04 (d, 3H, MeC(H)N, $^3J_{\text{HH}} = 6.8$ Hz), 1.00 (s, 3H, C(O)Me_a), 0.97 (s, 3H, C(O)Me_b), 0.94 (s, 3H, C(O)Me_c), 0.70 (s, 3H, C(O)Me_d). $^{13}\text{C}\{^1\text{H}\}$ NMR (5:1 d_6 -benzene– d_8 -THF): δ 150.8, 150.4 (br), 149.2, 147.8 (br), 138.4 (br), 135.8 (br), 133.7, 129.2, 128.4, 127.3, 125.8, 124.4, 122.9 (aryl *C*); 78.0, 77.1 (ZrOC_{ab}); 61.0 (MeC(H)N); 48.6, 47.4 (NCH_{2a,b}); 37.6, 37.2 (C(O)C_{ab}H₂); 31.7, 31.6, 30.2, 29.0 (C(O)Me); 31.5 (br, BCH₂); 7.5 (MeC(H)N); the fluorinated aryl carbons are not well-resolved in this solvent. $^{19}\text{F}\{^1\text{H}\}$ NMR (5:1 d_6 -benzene– d_8 -THF): δ −167.5 (t, 6F, *m* aryl *F*, $^3J_{\text{FF}} = 20$ Hz), −164.8 (t, 3F, *p* aryl *F*, $^3J_{\text{FF}} = 20$ Hz), −130.6 (d, 6F, *o* aryl *F*, $^3J_{\text{FF}} = 20$ Hz). The $^{19}\text{F}\{^1\text{H}\}$ NMR recorded in d_6 -benzene shows resonances at δ −166.9, −164.0, and −130.7 ppm. $^{13}\text{C}\{^1\text{H}\}$ NMR (d_5 -bromobenzene): δ 148.8 (d, $^1J_{\text{CF}} = 233$ Hz, aryl CF); 138.6 (br m, ipso aryl CF); 137.8 (d, $^1J_{\text{CF}} = 244$ Hz, aryl CF); 136.8 (d, $^1J_{\text{CF}} = 256$ Hz, aryl CF); 148.9, 137.7, 128.5, 127.4, 123.1, 122.8, 122.3 (aryl CH; others may be obscured by the solvent peaks); 81.1, 80.0 (C(O)Me₂); 59.1 (NCHMe); 50.3, 50.8 (NCH₂); 32.4 (br s, BCH₂); 31.6 (CH₂C(O)); only one peak is discernible); 14.6 (NCHMe).

Phenylacetylene Cyclotrimerization. In a typical NMR tube experiment, **7** (0.025 g, 0.053 mmol) and excess phenylacetylene (30 equiv) were dissolved in 0.8 mL of d_6 -benzene and the sample was heated at 70°C overnight. At this point the sample had darkened to brown and resonances due to phenylacetylene were no longer observable. The sample was quenched with H_2O , and the organic phase was extracted with Et_2O and washed with 1 M HCl. GC-MS showed that the major products in the organic fraction were 1,2,4- and 1,3,5-triphenylbenzene in a 3:1 ratio.

Table 1. Summary of Crystallographic Data

	7	8b
formula	C ₂₅ H ₃₅ NO ₂ Zr	C ₃₆ H ₄₃ NO ₃ Zr
fw	472.78	628.95
cryst syst	orthorhombic	orthorhombic
space group	<i>P</i> 2 ₁ 2 ₁ 2 ₁ (No. 19)	<i>P</i> 2 ₁ 2 ₁ 2 ₁ (No. 19)
<i>a</i> (Å)	9.795(2)	9.535(2)
<i>b</i> (Å)	11.246(2)	17.675(3)
<i>c</i> (Å)	22.910(3)	19.786(2)
$\alpha = \beta = \gamma$ (deg)	90	90
<i>V</i> (Å ³)	2523.5(9)	3334.4(9)
<i>Z</i>	4	4
ρ (calcd) (g cm ⁻³)	1.244	1.253
μ (cm ⁻¹)	37.4	29.8
radiation, λ (Å)	Cu K α , 1.542	Cu K α , 1.542
<i>T</i>	ambient	ambient
2 θ _{max} (deg)	100	110
no. of obsd rflns	1271	1647
no. of unique rflns	1525	2389
<i>R</i> ^a	0.062	0.050
<i>R</i> _w ^b	0.061	0.054

$$^a R = \sum(|F_o| - |F_c|)/\sum|F_o|. \quad ^b R_w = [\sum w(|F_o| - |F_c|)^2/\sum w(|F_o|)^2]^{1/2}.$$

Ethylene Polymerization. Polymerization experiments were carried out by saturating 450 mL of toluene with ethylene (75 psi). Separate samples of MAO cocatalyst (10.0 mmol) and complex (0.010 mmol) dissolved in 25 mL of toluene were added, and the reaction was monitored by observing the ethylene uptake. The product was isolated by removal of solvent, washed with hexane, and vacuum-dried. The amount of polyethylene was weighed, and the molecular weight and polydispersity were determined by GPC using a polyethylene standard. No significant polymerization was observed using an equimolar amount of B(C₆F₅)₃ as cocatalyst.

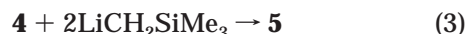
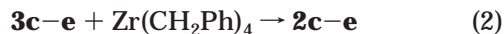
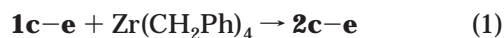
X-ray Crystallographic Studies. Crystallographic data for **7** and **8b** are given in Table 1. Crystals of each compound (**7**, 0.24 × 0.36 × 0.20 mm; **8b**, 0.20 × 0.22 × 0.20 mm) were loaded into glass capillaries in the glovebox and subsequently examined by photographic methods using Weissenberg and precession cameras. The space group (*P*2₁2₁2₁ in both cases) was uniquely determined by the systematic absences. The crystals were transferred to a Nonius CAD4F diffractometer equipped with Ni-filtered Cu K α radiation. The unit cells were refined using 25 reflections in the 2 θ ranges 50–75° (**7**) and 48–85° (**8b**). Experimental densities were not determined because of the air and moisture sensitivity of the compounds. Three standard reflections, measured periodically during data collection (**7**, 400, 040, and 004; **8b**, 104, 400, and 140), showed less than a 2% decline in combined intensity for both compounds. Intensity measurements were collected for one-fourth of the sphere. After the usual data reduction procedures,^{14a} the structures were solved using Patterson methods. The refinements minimized $\sum w(|F_o| - |F_c|)^2$ and proceeded normally using SHELX86.^{14b} The criterion for inclusion of reflections was $I > 2.5\sigma(I)$ for **7** and $I > 3.0\sigma(I)$ for **8b**. The weighting scheme was determined by counting statistics using $w = 1/(\sigma^2(F) + 0.001(F^2))$. Convergence was satisfactory: max shift/esd = 0.005. A total of 262 parameters (29 × 9 parameters per atom + scale) were refined for **7** and 370 parameters (41 atoms × 9 parameters per atom + scale) for **8b**. No intermolecular contacts shorter than 3.4 Å were observed in either case. The benzene ring of the benzyl group in **7** was refined with bond length constraints and is drawn isotropically in the ORTEP plot for clarity.¹⁵ Structural plots were drawn with ORTEP or the ZORTEP modification.¹⁶

(13) For a similar structure see: Stephan, D. W. *Organometallics* **1990**, *9*, 2718.

(14) (a) Larson, A.; Lee, F.; Page, Y.; Webster, M.; Charland, J.; Gabe, E. J. NRC Solver: A Program for Crystal Structure Determination; National Research Council of Canada, Chemistry Division, Ottawa, ON, Canada, 1985. (b) Sheldrick, G. M. SHELX86, Programs for Crystal Structure Determination; University of Cambridge, Cambridge, U.K., 1986.

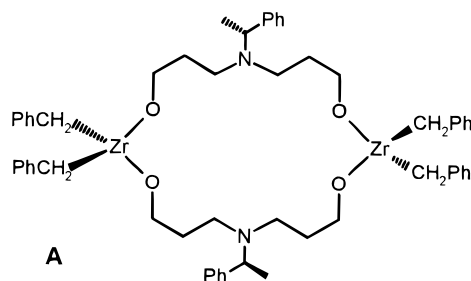
Results and Discussion

Synthesis of (Aminodiolate)zirconium Dialkyl Complexes. The zirconium dialkyl complexes **2** were prepared by three different routes: hydrocarbon elimination (protonolysis), ligand redistribution, or metathesis (eqs 1–3).



Direct reaction of aminodiolols **1c–e** with tetrabenzylzirconium afforded dibenzyl complexes **2c–e** in excellent yield and high purity. This method works well for the bulkier aminodiolols, but the formation of bis(ligand) complexes is difficult to avoid with **1a,b**. Complex **2b** can be prepared cleanly by slow addition of a dilute solution of **1b** to tetrabenzylzirconium at –78 °C. Using the same strategy for the preparation of **2a** produced a product that inevitably contained significant amounts of the bis(ligand) complex Zr{MeN(CH₂CH₂C(O)Me₂)₂}₂ (**3a**).¹² Attempts to purify **2a** by recrystallization were unsuccessful because of the similarity in solubilities of **2a** and the bis(ligand) complex.

Ligand redistribution between tetrabenzylzirconium and the previously prepared bis(ligand) complexes **3c–e** also affords **2c–e** in excellent yield and purity. Complexes **3c,d**, containing *tert*-butyl-substituted ligands, undergo very rapid (<1 min) redistribution, and neither starting material nor intermediate are observable by NMR immediately after mixing. Redistribution with **3e** is slower, and an intermediate is observable by ¹H NMR. The region characteristic of the α -methylbenzyl CH proton resonance (3.9–4.4 ppm) was monitored by ¹H NMR over a period of 3 h (Figure 1). Shortly after mixing, resonances due to **3e**, **2e**, and the intermediate **A** were observed. After 30 min, the broad resonance due



to **3e** had vanished while that of the intermediate was just discernible. Over the following 2 h, the resonance due to **A** disappeared, leaving only that due to **2e**. Although the identity of **A** is not known with certainty, a symmetrically bridged structure such as that shown is reasonable.¹³

In contrast to **3c–e**, the *N*-methyl-substituted complexes **3a** and Zr{MeN(CH₂CH₂C(O)Ph₂)₂}₂ (**3b**) do not undergo ligand redistribution with tetrabenzylzirconium, even when heated to 70 °C in benzene for prolonged periods of time. In other work¹² we showed

(15) Johnson, C. K. ORTEPII; Oak Ridge National Laboratory, Oak Ridge, TN, 1976.

(16) Zsolnai, L. ZORTEP; University of Heidelberg, Heidelberg, Germany, 1995.

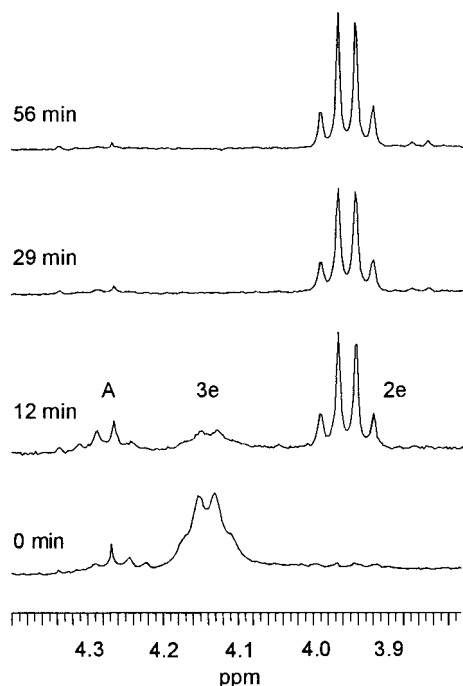
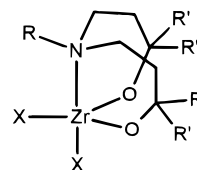


Figure 1. ^1H NMR spectra (360 MHz) of the α -methylbenzyl CH proton region as a function of time for the ligand redistribution reaction between $\text{Zr}[\text{N}(\text{CH}_2\text{CH}_2\text{C}(\text{O})\text{Me}_2)_2]\{((S)\text{-PhC}(\text{H})\text{Me})\}_2$ (**3e**) and $\text{Zr}(\text{CH}_2\text{Ph})_4$ in d_6 -benzene. Resonances due to $\text{Zr}[\text{N}(\text{CH}_2\text{CH}_2\text{C}(\text{O})\text{Me}_2)_2]\{((S)\text{-PhC}(\text{H})\text{Me})\}_2[\text{CH}_2\text{Ph}]_2$ (**2e**) and the unknown intermediate **A** are observed shortly after mixing.

that these same complexes undergo arm exchange via amine dissociation, inversion at nitrogen, and recoordination much more slowly than **3c–e**. This was attributed to stronger amine binding for **3a,b**, and since amine dissociation is likely to be a prerequisite for formation of a bridged complex such as **A**, it is not surprising that these two effects are related.

The first two preparative routes are not general because they are limited to available zirconium tetraalkyls. Since a more general route is desirable, the preparation of the dichlorides was also briefly investigated. Addition of aminodiols **1b** to $\text{ZrCl}_2[\text{N}(\text{SiMe}_3)_2]_2$ in toluene resulted in formation of a white insoluble precipitate, presumed to be the dihalide **4**. Reaction of **4** with 2 equiv of benzylpotassium or ((trimethylsilyl)methyl)lithium resulted in chain formation of **2b** and $\text{Zr}\{\text{MeN}(\text{CH}_2\text{CH}_2\text{C}(\text{O})\text{Ph}_2)_2\}[\text{CH}_2\text{SiMe}_3]_2$ (**5**), respectively, although the former was obtained in lower yield than by hydrocarbon elimination. A similar reaction between **4** and methyllithium produced $\text{Zr}\{\text{MeN}(\text{CH}_2\text{CH}_2\text{C}(\text{O})\text{Ph}_2)_2\}\text{Me}_2$ (**6**), but the thermal sensitivity of this product precluded isolation of the pure complex.

Solution Structures. The ^1H NMR spectra of **2a,b**, **5**, and **6** show that these complexes are conformationally rigid in d_6 -benzene at room temperature. For each, resonances due to two inequivalent sets of alkyl ligands and one alkoxide arm are observed; however, the geminal protons of the alkoxide arms are inequivalent, indicating mirror plane (C_s) symmetry. These observations are consistent with the *pseudo-fac* trigonal bipyramidal structures shown. This structure is consistent with our earlier observation that the aminodiolate ligands prefer to adopt *fac* coordination sites in the six-coordinate bis(ligand) complexes.¹² This structure is also



	R	R'	X
2	a	Me	Benzyl (Bz)
	b	Ph	Bz
	c	Me	Bz
	d	Ph	Bz
	e	(S)-PhC(H)Me	Bz
4	Me	Ph	Cl
5	Me	Ph	CH_2SiMe_3
6	Me	Ph	Me

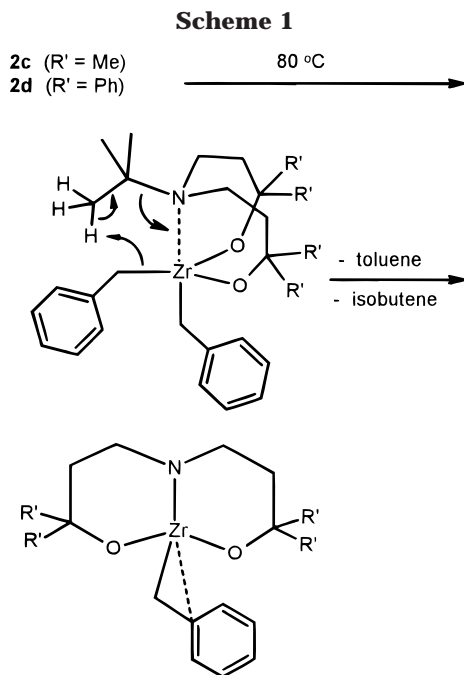
very similar to that observed by Horton et al.^{17c} for zirconium dialkyl complexes of the chelating aminodiols $\text{Me}_3\text{SiN}(\text{CH}_2\text{CH}_2\text{N}(\text{SiMe}_3)_2)_2$.¹⁷ There is no evidence from ^1H NMR to suggest that any of these complexes involve η^2 -benzyl coordination.^{17c,18}

In contrast to the dialkyls discussed above, **2c–e** are fluxional at room temperature, showing a single type of benzyl group and only one set of resonances for each chemically distinct CH_2 group of the ligand backbone. This fluxional behavior can again be accounted for by amine dissociation and inversion at nitrogen followed by amine recoordination as discussed previously.¹² Indeed, cooling **2d** to -60°C results in splitting of the CH_2 and $\text{C}(\text{O})\text{R}_2$ resonances into two groups consistent with C_s symmetry. However, the benzyl groups remain equivalent to -80°C , suggesting that pseudorotation remains rapid even at low temperatures.

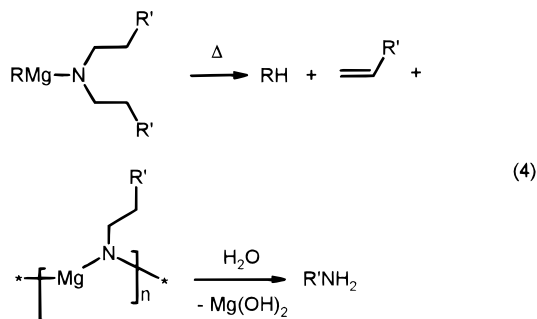
Thermal Stability. The thermal stabilities of **2a–e** show a marked dependence on the substituent at nitrogen. The methyl complex **2b** survives unchanged after heating for 5 days at 100°C in d_8 -toluene. In contrast, the *tert*-butyl derivatives **2c,d** decompose by elimination of isobutene and toluene (Scheme 1). Conclusive NMR evidence for the formation of $\text{Zr}[\text{N}(\text{CH}_2\text{CH}_2\text{C}(\text{O})\text{R}'_2)_2][\text{CH}_2\text{Ph}]$ could not be obtained, possibly because of secondary decomposition processes. The decomposition reaction of **2d**, monitored by NMR, was found to be first order in the starting dibenzyl complex. An Eyring plot (Figure 2) gave ΔH^\ddagger and ΔS^\ddagger values of $26 \pm 2 \text{ kcal mol}^{-1}$ and $-11 \pm 1 \text{ cal mol}^{-1} \text{ K}^{-1}$ for this decomposition reaction. The negative value of ΔS^\ddagger is consistent with the highly ordered transition state depicted in Scheme 1. Decomposition of the less crowded

(17) (a) Cloke, F. G. N.; Hitchcock, P. B.; Love, J. B. *J. Chem. Soc., Dalton Trans.* **1995**, 25. (b) Clark, H. C. S.; Cloke, F. G. N.; Hitchcock, P. B.; Love, J. B.; Wainwright, A. P. *J. Organomet. Chem.* **1995**, 501, 333. (c) Horton, A. D.; de With, J.; van der Linden, A. J.; van de Weg, H. *Organometallics* **1996**, 15, 2672.

(18) Typically η^2 -benzyl groups display characteristic NMR features including an upfield shift of the ortho benzyl protons (ca. 6.0–6.7 ppm) and ipso benzyl carbon (ca. 10 ppm upfield), an increased benzylic CH coupling constant ($^1J_{\text{CH}} > 125 \text{ Hz}$), and a decreased benzylic HH coupling constant ($^2J_{\text{HH}} < 10 \text{ Hz}$).^{18e} (a) Latesky, S. L.; McMullen, A. K.; Nicolai, G. P.; Rothwell, I. P.; Huffman, J. C. *Organometallics* **1985**, 4, 902. (b) Bochmann, M.; Lancaster, S. J. *Organometallics* **1993**, 12, 633. (c) Bochmann, M.; Lancaster, S. J.; Hursthouse, M. B.; Malik, K. M. A. *Organometallics* **1994**, 13, 2235. (d) Jordan, R. F.; LaPointe, R. E.; Bajgur, C. S.; Echolls, S. F.; Willet, R. *J. Am. Chem. Soc.* **1987**, 109, 4111. (e) We thank one reviewer for pointing out the significance of the $^2J_{\text{HH}}$ values.

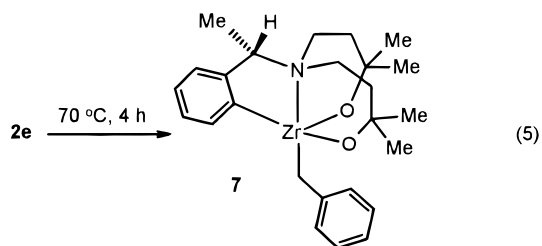


complex **2c** proceeded at roughly one-fifth the rate for **2d**, suggesting that relief of steric pressure is an important driving force in the decomposition reaction. Thermal dealkylation, similar to that shown in Scheme 1, has been used as a method for the preparation of primary amines from the corresponding metal amides (eq 4).¹⁹ The negative entropies of activation observed



during alkene elimination according to eq 4 were taken as evidence for a concerted cyclic transition state.¹⁹ Isobutene elimination from *tert*-butylamine has been reported in the literature by both radical²⁰ and ionic²¹ mechanisms.

Chiral complex **2e** undergoes clean ortho metalation during mild heating (70 °C, 4 h) in *d*₆-benzene to afford metallacycle **7** in 75% yield (eq 5). The structure of **7**



was suggested by NMR spectroscopy and confirmed by

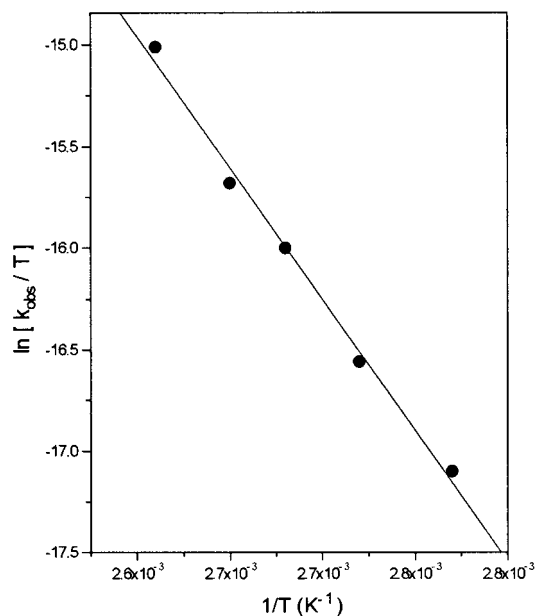


Figure 2. Eyring plot for the thermal decomposition of $\text{Zr}[t\text{-BuN}(\text{CH}_2\text{CH}_2\text{C}(\text{O})\text{Ph})_2][\text{CH}_2\text{Ph}]_2$ (**2d**).

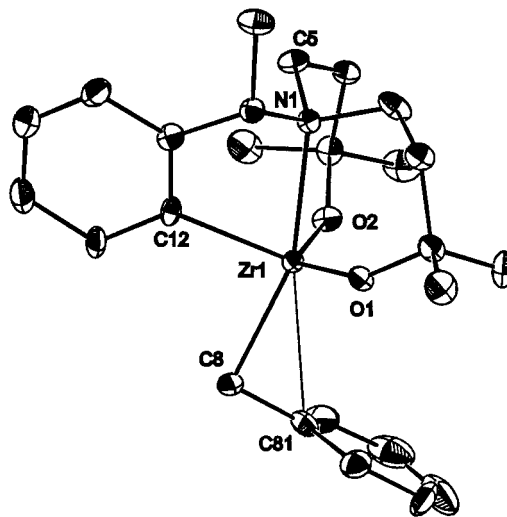


Figure 3. ZORTEP¹⁶ plot (30% probability) of $\text{Zr}[\text{N}\{\text{CH}_2\text{-CH}_2\text{C}(\text{O})\text{Me}\}_2\{((S)\text{-}2\text{-C}_6\text{H}_4\text{C}(\text{H})\text{Me})\}][\text{CH}_2\text{Ph}]$ (**7**).

a single-crystal X-ray investigation. The structure, depicted in Figure 3, consists of a pseudo-trigonal-bipyramidal geometry with the coordinated amine and remaining benzyl CH_2 group occupying the axial positions ($\text{N}(1)\text{-Zr}(1)\text{-C}(8)$ angle $159.1(6)^\circ$). The two alkoxide oxygens and the ortho-metallated phenyl carbon occupy the equatorial sites with the $\text{O-Zr-C}(\text{aryl})$ angles ($110.7(5)$ and $112.8(5)^\circ$) compressed substantially relative to the O-Zr-O angle ($125.4(4)^\circ$). Selected bond distances and angles are collected in Table 2.

The η^2 -benzyl group of **7** is clearly evident from the $\text{Zr}(1)\text{-C}(8)\text{-C}(81)$ angle of $93.4(11)^\circ$ and the short $\text{Zr}(1)\text{-C}(81)$ contact of $2.817(19)$ Å. While η^2 -benzyl groups are commonly observed for electron-deficient early-transition-metal complexes,^{17c,18,22} this result stands in contrast to the η^1 -benzyl bonding observed for **2b**. Since the electronic environments at zirconium in **2b** and **7**

(20) Patai, S., Ed. *Chemistry of the Amino Group*, Wiley-Interscience: London, 1968; p 437.

(21) Ainsworth, C.; Easton, N. R. *J. Org. Chem.* **1962**, *27*, 4118.

(19) Ashby, E. C.; Willard, G. F. *J. Org. Chem.* **1978**, *43*, 4750.

Table 2. Selected Bond Distances (Å) and Angles (deg) for **7**^a

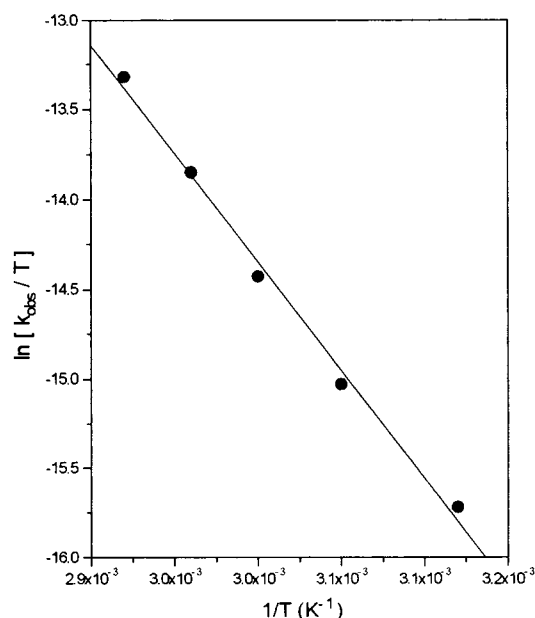
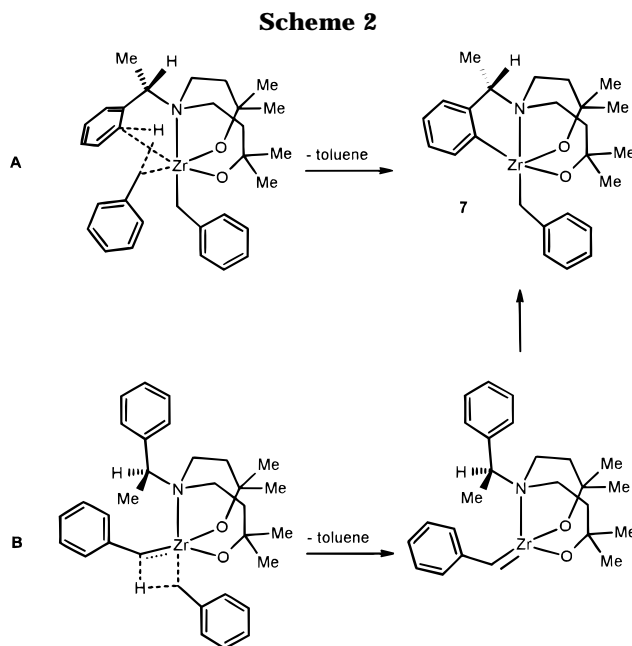
Distances			
Zr(1)–N(1)	2.149(12)	N(1)–C(1)	1.43(2)
Zr(1)–O(1)	1.938(9)	O(1)–C(4)	1.40(2)
Zr(1)–O(2)	1.927(10)	O(2)–C(7)	1.39(2)
Zr(1)–C(8)	2.313(16)	C(1)–C(11)	1.54(2)
Zr(1)–C(12)	2.275(14)	C(8)–C(81)	1.48(2)
Zr(1)–C(81)	2.82(2)	C(11)–C(12)	1.39(2)
Angles			
N(1)–Zr(1)–O(1)	81.0(5)	O(2)–Zr(1)–C(8)	105.9(8)
N(1)–Zr(1)–O(2)	82.8(5)	O(2)–Zr(1)–C(12)	110.7(5)
N(1)–Zr(1)–C(8)	159.1(6)	C(8)–Zr(1)–C(12)	87.4(6)
N(1)–Zr(1)–C(12)	71.7(5)	Zr(1)–C(8)–C(81)	93.4(11)
O(1)–Zr(1)–O(2)	125.4(4)	Zr(1)–O(1)–C(4)	140.4(10)
O(1)–Zr(1)–C(8)	107.5(8)	Zr(1)–O(2)–C(7)	145.2(10)
O(1)–Zr(1)–C(12)	112.8(5)	Zr(1)–C(12)–C(11)	115.8(12)

^a Estimated standard deviations in parentheses.

must be very similar, the observation of η^1 -benzyl coordination in **2b** is probably steric in origin. Interestingly, while **7** does display some of the NMR features normally associated with η^2 -benzyl coordination in solution (benzyl ipso aryl ^{13}C resonance, 144.1 ppm; benzyl CH_2 $^1J_{\text{CH}} = 131$ Hz and $^2J_{\text{HH}} = 9.1$ Hz), the ortho aryl ^1H resonances appear in the region normally associated with η^1 coordination (δ 7.35 ppm).¹⁸ This suggests to us that if an η^2 -benzyl interaction is present in solution, it is quite weak. Certainly, stronger η^2 -benzyl bonding has been observed for related compounds; for example, one benzyl group in $\text{Zr}(\text{OAr}')(\text{CH}_2\text{-Ph})_3$ ($\text{OAr}' = 2,6\text{-di-}t\text{-butylphenoxide}$) shows a more acute $\text{Zr}-\text{CH}_2-\text{C}(\text{ipso})$ angle (84°) and a shorter $\text{Zr}-\text{C}(\text{ipso})$ bond distance (2.64 Å).^{18a}

The Zr–O bond distances in **7** are unexceptional, but the alkoxide Zr–O–C angles ($140.4(10)$ and $145.2(10)^\circ$) are considerably more bent than that found in $\text{Zr}(\text{OAr}')(\text{CH}_2\text{Ph})_3$ ($165.7(9)^\circ$)^{18a} or those for the terminal alkoxides of $[(i\text{-PrO})_3(i\text{-PrOH})\text{Zr}(\mu\text{-}i\text{-PrO})_2]$ (mean 172°).²³ This is not surprising, because bending at the alkoxide oxygens is necessary if the chelating ligand is to bind to a single metal center. The Zr–N distance of 2.419(12) Å is short in comparison to that found for the structurally similar $\text{Zr}[(\text{Me}_3\text{Si})\text{N}(\text{CH}_2\text{CH}_2\text{NSiMe}_3)_2][\text{CH}(\text{SiMe}_3)_2][\text{Cl}]$ (2.770(5) Å).^{17a} The short Zr–N distance in **7** is due to formation of the five-membered ring involving the ortho-metalated phenyl group. Similarly, exceptionally short Ti–N distances have been observed in titanium complexes bearing deprotonated triethanolamine as a tripodal ligand (the titanatranes).⁶

The formation of **7** was found to follow first-order kinetics, consistent with an intramolecular process, and an Eyring plot (Figure 4) yielded ΔH^\ddagger and ΔS^\ddagger values of 24 ± 2 kcal mol^{−1} and -5 ± 1 cal mol^{−1} K^{−1}, respectively. The two most likely pathways for metalacycle formation are via direct σ -bond metathesis (**A**) or via a benzyldiene intermediate (**B**) (Scheme 2).^{24,25}

**Figure 4.** Eyring plot for the formation of **7** by ortho metalation.

In an elegant study, Bercaw²⁶ showed conclusively that the closely related conversion of $\text{Cp}^*_2\text{Hf}(\text{CH}_2\text{C}_6\text{H}_5)_2$ to $\text{Cp}^*_2\text{Hf}(\text{CH}_2\text{-}o\text{-C}_6\text{H}_4)$ proceeded through a benzyldiene intermediate and an isolable “tuck” complex, $\text{Cp}^*\text{Hf}(\eta^5\text{-}\eta^1\text{-C}_5\text{Me}_4\text{CH}_2)(\text{CH}_2\text{C}_6\text{H}_5)$. Significantly, the entropy of activation of 1 ± 3 cal mol^{−1} K^{−1} for this reaction is similar to that observed for the formation of **7**. In contrast, most examples of direct σ -bond metathesis exhibit substantially more negative entropies of activation ($\Delta S^\ddagger = -10$ to -24 cal mol^{−1} K^{−1}),²⁷ which has been

(22) (a) Jordan, R. F.; LaPointe, R. E.; Baenziger, N. C.; Hinch, G. D. *Organometallics* **1990**, 9, 1539. (b) Dais, G. R.; Jarvis, J. A.; Kilburn, B. T.; Piols, A. J. P. *J. Chem. Soc., Chem. Commun.* **1971**, 677. (c) Davis, G. R.; Jarvis, J. A.; Kilburn, B. T. *J. Chem. Soc., Chem. Commun.* **1971**, 1511. (d) Mintz, E. A.; Moloy, K. G.; Marks, T. J. *J. Am. Chem. Soc.* **1982**, 104, 4692.

(23) Vaarstra, B. A.; Huffman, J. C.; Gradeff, P. S.; Hubert-Pfalzgraf, L. G.; Daran, J.; Parraud, S.; Yunlu, K.; Caulton, K. G. *Inorg. Chem.* **1990**, 29, 3126.

(24) Initial metalation at sites other than the ortho phenyl position followed by subsequent metalation at this site is also possible. These alternatives can be ruled out by labeling studies (vide infra).

(25) Fryzuk, M. D.; Mao, S. S. H.; Zaworotko, M. J.; MacGillivray, L. R. *J. Am. Chem. Soc.* **1993**, 115, 5336.

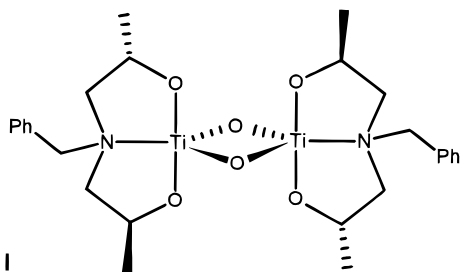
(26) Bulls, A. R.; Schaefer, W. P.; Serfas, M.; Bercaw, J. E. *Organometallics* **1987**, 6, 1219.

(27) (a) Rothwell, I. P. *Polyhedron* **1985**, 4, 177. (b) Smith, G. M.; Carpenter, J. D.; Marks, T. J. *J. Am. Chem. Soc.* **1986**, 108, 6805. (c) Bruno, J. W.; Smith, G. M.; Marks, T. J.; Fair, C. K.; Schultz, A. J.; Williams, J. M. *J. Am. Chem. Soc.* **1986**, 108, 40. (d) Sock, L. E.; Brock, C. P.; Marks, T. J. *Organometallics* **1987**, 6, 232. (e) Luinstra, G. A.; Teuben, J. H. *Organometallics* **1992**, 11, 1793.

attributed to the formation of a highly ordered four-center transition state. However, while entropies of activation values are sometimes suggestive of a mechanistic pathway, they are not infallible guides. With regard to the present reaction there are, for example, reactions proceeding via an alkylidene which exhibit large negative entropies of activation²⁸ and others for which an alkylidene is highly unlikely which show very small activation entropy.²⁹ Fryzuk's study of the thermal decomposition of $Y[N(\text{SiMe}_2\text{CH}_2\text{PMe}_2)_2](\text{CH}_2\text{C}_6\text{H}_5)$ is a particularly relevant example of the latter case.²⁹ In this reaction, intramolecular metalation occurs exclusively at the CH_2 site adjacent to P with elimination of toluene ($\Delta S^\ddagger = -3 \pm 3 \text{ cal mol}^{-1} \text{ K}^{-1}$). To accommodate the exceptionally small ΔS^\ddagger value, the authors postulated that phosphine dissociation occurs in the transition state to provide a positive contribution to ΔS^\ddagger . Since amine dissociation could similarly occur in the transition state leading to **7**, it would be premature to rule out a σ -bond metathesis pathway.

To establish the decomposition mechanism unequivocally, two separate isotopic labeling experiments were carried out. The labeled compounds **2e** (d_7 -benzyl)₂ and **2e** (o - d_2 -PhC(Me)H) were prepared by reaction of **1e** with $\text{Zr}(\text{CD}_2\text{C}_6\text{D}_5)_4$ and of **1e** (o - d_2 -PhC(Me)H)³⁰ with $\text{Zr}(\text{CH}_2\text{-Ph})_4$, respectively. Thermolysis of the labeled compounds in d_6 -benzene (4 h, 70 °C) was monitored by ¹H NMR. In both cases, the NMR spectra showed no evidence for H–D scrambling and the toluene produced was identified as exclusively d_7 -(CD₂H)C₆D₅ in the first experiment and d -(CDH₂)C₆H₅ in the second. These results conclusively rule out involvement of a benzylidene pathway, because in both cases this would necessarily lead to H–D scrambling (Scheme 2). A metathesis pathway involving any sites other than the ortho aryl protons of the phenyl ligand may also be ruled out, because this would not result in the exclusive formation of the d -(CDH₂)C₆H₅ in the second experiment. The direct σ -bond metathesis pathway is the only possibility that explains these results.

Reactivity Studies. (a) Insertion Chemistry of Aldehydes and Ketones with 7. Chiral group 4 alkoxides have been successfully used for enantioselective alkylations of aldehydes and ketones with lithium reagents. In one example, closely related to the types of complexes described here, Nugent reported that 5 mol % of **1** functions as an excellent enantioselective catalyst

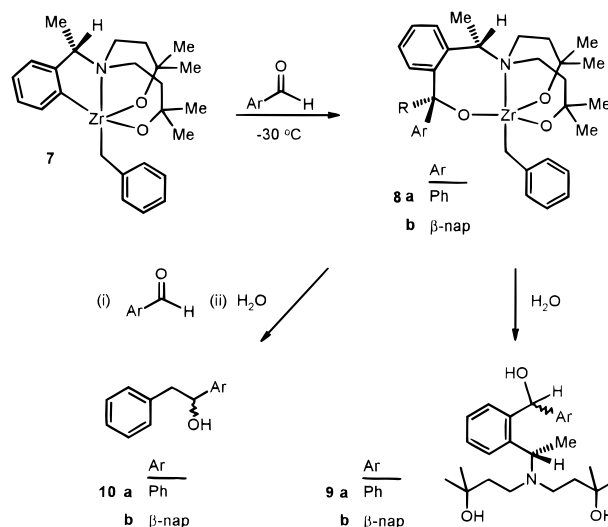


(28) (a) Cheon, J.; Rogers, D. W.; Girolami, G. *J. Am. Chem. Soc.* **1997**, *119*, 6804. (b) Li, L.; Hung, M.; Xue, Z. *J. Am. Chem. Soc.* **1995**, *117*, 12746. (c) van der Heijden, H.; Hessen, B. *J. Chem. Soc., Chem. Commun.* **1995**, 145.

(29) Fryzuk, M. D.; Haddad, T. S.; Rettig, S. J. *Organometallics* **1991**, *10*, 2026.

(30) Ortho deuteration of **1e** was achieved by repetitive quenching of **8** with D₂O. Three cycles were sufficient to give >90% o - d_2 -**1e**.

Scheme 3



for the alkylation of benzaldehyde with diethylzinc (96% ee).³¹ Since **7** is enantiomerically pure, albeit with a chiral center remote to the zirconium–carbon bond, an investigation of the regio- and stereoselectivity of C=O insertion was warranted.

Reaction of 1 equiv of benzaldehyde or β -naphthaldehyde with **7** at -30 °C resulted in exclusive insertion of the carbonyl group into the phenyl–zirconium bond (Scheme 3). The insertion products **9a**, **b** were isolated as pure oils after hydrolysis and were identified by NMR spectroscopy. In all three cases, the major diastereomer (>85% de) was identified as the *RS* isomer by a combination of NOE difference experiments and molecular modeling;³² this absolute configuration was confirmed for the zirconium complex **8b** by X-ray crystallography (vide infra).

The regioselectivity of this first insertion is interesting since, in the case of lithium reagents at least, benzyl–metal bonds are generally more reactive³³ in addition reactions with carbon–carbon and carbon–oxygen double bonds. In the present system, we have found that the benzyl–carbon bond in **7** is a better base in reactions

(31) Nugent, W. A. *J. Am. Chem. Soc.* **1992**, *114*, 2768.

(32) Molecular modeling (CAShe) of the free ligand **9b** was used to establish the distance between the PhC(H)N and CH(OH) protons for each diastereomer. The PhC(H)N resonance showing the greatest relative NOE effect upon irradiation of the related CH(OH) proton was assigned as the *SR* diastereomer, because this isomer was calculated to have the shortest proton–proton distance (2.1 versus 2.3 Å for the *SS* diastereomer). The major isomer of **9a** was also assigned as the *SR* diastereomers on the basis of the strong similarity of the NMR spectrum to that of the major isomer of **9b**.

(33) In most cases, the relative rate of addition by lithium reagents is opposite that predicted on the basis of anion basicity; that is, the least basic carbanion reacts fastest with the substrate. For example, the relative addition rates of benzyl lithium and phenyllithium to 1,1-diphenylethene in THF were reported to be more than 3000:1.^{33a,b} The relative rate of addition of phenyllithium and ethyllithium to Michler's ketone (4,4'-dimethylaminobenzophenone) was reported as 3:1 in THF; the rate of addition of benzyl lithium was not reported.^{33c} Interestingly, the relative rate of deprotonation of triphenylmethane by RLi in THF follows the order benzyl (250) > phenyl (5.5) > Me (1.0).^{33d} Solvation effects and the degree of aggregation in solution no doubt play a role in this order, but it is clear that it is not straightforward to predict the relative reactivity of benzylic and phenyl carbanions on the basis of simple anion stability arguments: (a) Waack, R.; Doran, M. A. *J. Am. Chem. Soc.* **1969**, *91*, 2456. (b) Waack, R.; Doran, M. A. *J. Org. Chem.* **1967**, *32*, 3395. (c) Swain, C. G.; Kent, L. *J. Am. Chem. Soc.* **1950**, *72*, 518. (d) Waack, R.; West, P. *J. Am. Chem. Soc.* **1964**, *86*, 4494.

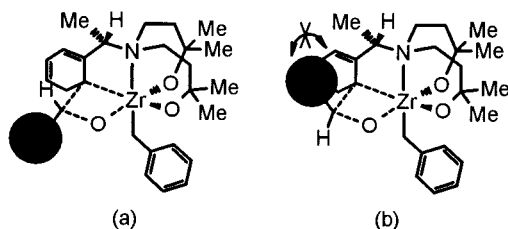


Figure 5. Possible transition state geometries for aldehyde insertion into the Zr–phenyl bond of **7**.

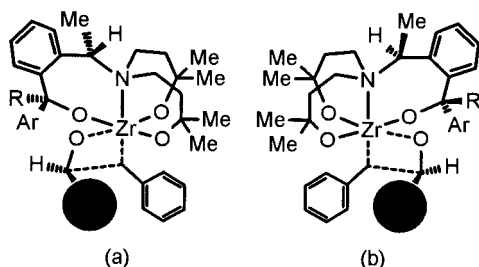


Figure 6. Possible transition state geometries for the insertion of a second equivalent of aldehyde into the benzyl–Zr bond of **8b**.

with primary amines.³⁴ The stereochemistry of the insertion can be understood if it is assumed that the substrate binds preferentially at the site opposite the α -methyl substituent of the metalated α -methylbenzyl group (Figure 5). In this site, there will be a strong steric preference favoring nucleophilic attack at the enantiotopic face of the substrate shown in Figure 5a (leading to an *R* configuration at the newly formed chiral center). Presentation of the opposite enantiotopic face of the substrate (Figure 5b) would place the substrate aryl group in close proximity with the ligand backbone. In view of this interaction, it seems more likely that the minor (*SS*) isomer is formed by coordination of the substrate in the same orientation as shown in Figure 5a but at the site on the same side as the α -methyl substituent, thus exposing the opposite enantiotopic face to nucleophilic attack.

Addition of a second equivalent of benzaldehyde or β -naphthaldehyde to **7** resulted in insertion into the Zr–benzyl bond after warming to room temperature. The products **10a,b** were identified after hydrolysis by ¹H NMR. Chiral shift reagents showed that both products were formed in approximately 45% ee; the absolute configuration of the major and minor enantiomers was not determined. The lower stereoselectivity for the second insertion can probably be traced to the orientation of the aldehyde plane in Figure 6. Even assuming that an orientation with the substrate aryl group lying near the ligand alkoxide groups is strongly preferred (Figure 6a), coordination on the same side as the α -methyl group will again expose the opposite enantiotopic face (Figure 6b). However, since the orientation of the aldehyde plane is now perpendicular to that during Zr–phenyl insertion (Figure 5), steric interactions with the α -methyl group are expected to be much less significant. Therefore, the transition states shown in Figure 6 are likely to be closer in energy than those in Figure 5 and less differentiation is expected to occur.

(34) Aniline or *tert*-butylamine (1 equiv) reacts with **7** to yield the metallacyclic amides $\text{Zr}[\text{N}(\text{CH}_2\text{CH}_2\text{C}(\text{O})\text{Me}_2)_2\{((S)-2-\text{C}_6\text{H}_4\text{C}(\text{H})\text{Me})\}][\text{NHR}]$ (*R* = Ph, *t*-Bu). Shao, P.; Berg, D. J. Unpublished results.

Table 3. Selected Bond Distances (Å) and Angles (deg) for **8b**^a

Distances			
Zr(1)–N(1)	2.619(9)	O(2)–C(8)	1.387(18)
Zr(1)–O(1)	1.928(9)	O(3)–C(19)	1.370(19)
Zr(1)–O(2)	1.917(9)	C(18)–C(19)	1.49(2)
Zr(1)–O(3)	1.945(10)	C(19)–C(20)	1.52(2)
Zr(1)–C(30)	2.284(15)	C(30)–C(31)	1.45(3)
O(1)–C(1)	1.429(19)		
Angles			
N(1)–Zr(1)–O(1)	81.0(4)	Zr(1)–N(1)–C(11)	111.3(8)
N(1)–Zr(1)–O(2)	80.3(4)	Zr(1)–O(1)–C(1)	147.4(10)
N(1)–Zr(1)–O(3)	84.5(3)	Zr(1)–O(2)–C(8)	151.4(10)
N(1)–Zr(1)–C(30)	179.2(4)	Zr(1)–O(3)–C(19)	161.1(9)
O(1)–Zr(1)–O(2)	119.8(4)	Zr(1)–C(30)–C(31)	110.2(11)
O(1)–Zr(1)–O(3)	119.8(4)	N(1)–C(11)–C(13)	112.8(14)
O(1)–Zr(1)–C(30)	99.4(6)	O(3)–C(19)–C(18)	110.6(13)
O(2)–Zr(1)–O(3)	114.5(4)	O(3)–C(19)–C(20)	112.7(13)
O(2)–Zr(1)–C(30)	98.9(5)	C(11)–C(13)–C(18)	122.7(15)
O(3)–Zr(1)–C(30)	95.8(5)	C(13)–C(18)–C(19)	120.4(14)

^a Estimated standard deviations in parentheses.

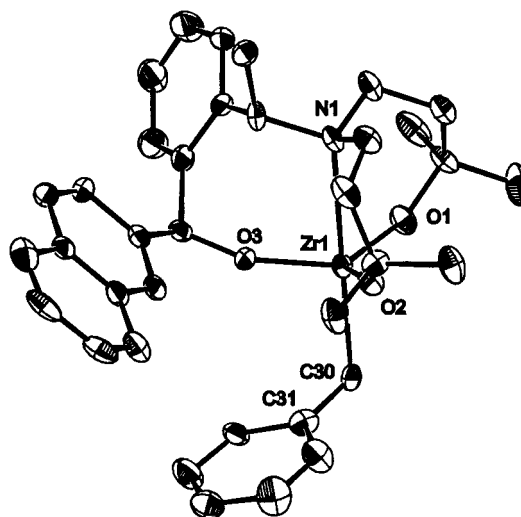
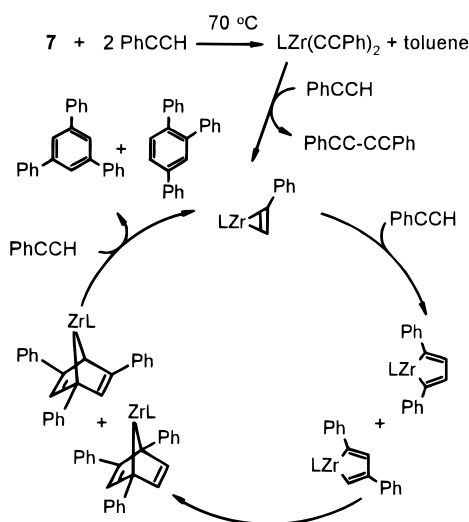


Figure 7. ZORTEP¹⁶ plot (30% probability) of $\text{Zr}[\text{N}(\text{CH}_2\text{CH}_2\text{C}(\text{O})\text{Me}_2)_2\{((S)-2-(R-(\beta\text{-naphthyl})\text{CH}(\text{O}))-C_6\text{H}_4\text{C}(\text{H})\text{Me})\}][\text{CH}_2\text{Ph}]$ (**8b**).

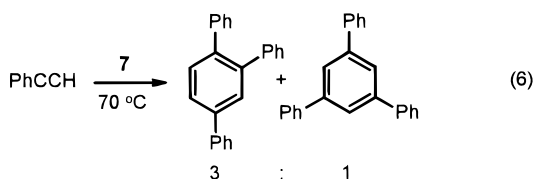
The structure of **8b** was confirmed by X-ray crystallography. Selected bond lengths and angles are collected in Table 3, while the structure is shown in Figure 7. Complex **8b** is distorted trigonal bipyramidal in geometry with the three alkoxide groups occupying the equatorial sites. The Zr–O bond lengths are quite similar to one another and to those observed for **7**. However, in contrast to **7**, the benzyl group of **8b** is clearly η^1 bound ($\text{Zr}(1)\text{--C}(30)\text{--C}(31) = 110.2(11)^\circ$). This is most likely the result of increased steric crowding in **8b**, although decreased metal Lewis acidity due to an increase in the number of alkoxide donors may also play a role. The compressed $\text{O}(1)\text{--Zr}(1)\text{--O}(2)$ angle ($119.8(4)^\circ$) relative to the more open alkoxide angle in **7** ($125.4(4)^\circ$) provides additional evidence for steric crowding in **8b**.

(b) Alkyne Cyclotrimerization with 7. Catalytic cyclotrimerization of alkynes is well-known for late-transition-metal complexes,³⁵ but fewer examples are known with early-metal catalysts.³⁶ This appears to stem in part from the fact that metallocene derivatives, by far the most heavily investigated class of complexes, do not appear to catalyze this reaction.^{3c} Rothwell has shown that titanium(IV) aryloxides of the type Ti-

Scheme 4



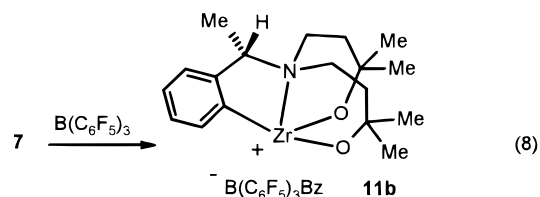
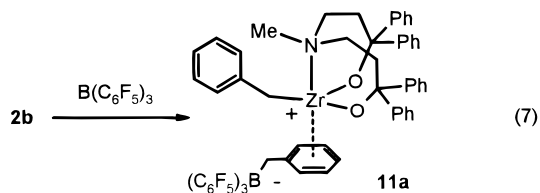
(OAr')₂Cl₂ (OAr' = 2,6-di-*tert*-butylphenoxide) must be reduced to Ti(II) in order to function as active catalysts.^{5c} More recently, Schaverien has demonstrated that zirconium dialkyl complexes supported by binaphtholate (BINOL) ligands function as highly active catalysts without preactivation.^{5a} Similarly, treatment of **7** with phenylacetylene at 70 °C leads to slow catalytic production of 1,2,4- and 1,3,5-triphenylbenzene (eq 6, 3:1 ratio



by GC). Internal alkynes fail to react directly with **7** even at elevated temperatures. One possible catalytic cycle, based on that proposed earlier by Rothwell, could account for the observed cyclotrimerization activity (Scheme 4).^{5c} However, despite repeated attempts, we have been unable to establish the presence of even trace diphenylbutadiyne (or diphenylbutadiene) in the hydrolyzed reaction mixtures. Alternative mechanisms involving single site insertions are also possible, although linear alkyne oligomers might be expected if such a mechanism was operative, and we have no evidence for their formation either. It is also not clear why the cyclotrimerization catalyst derived from **7** is so much less active (ca. 2.5 turnovers/day at 70 °C) than that obtained from Zr(BINOL)(CH₂Ph)₂^{5a} (40 equiv in hours at 25 °C). It is possible that the four-coordinate zirconium center in the BINOL complex simply allows

greater substrate access to the metal center, although electronic effects due to the presence of an amine donor in **7** cannot be ruled out.

(c) Cationic Zirconium Alkyl Complexes. Treatment of **2b** or **7** with 1 equiv of the strong Lewis acid B(C₆F₅)₃ in toluene results in an immediate color change from pale yellow to bright yellow-orange with separation of the cations **11a,b** as orange oils (eqs 7 and 8). The



oils are insoluble in hexane but dissolve enough in aromatic hydrocarbons to allow NMR spectra to be recorded. In *d*₆-benzene **11a** has a very complex ¹H and ¹⁹F NMR spectrum, suggesting strong association of the B(C₆F₅)₃(CH₂Ph)[−] anion with the zirconium cation.³⁷ In contrast, the ¹⁹F NMR of **11b** shows three well-resolved resonances with a chemical shift difference (Δδ_{m,p}) of 2.9 ppm between the meta and para F signals, suggesting that the anion is not strongly coordinated in this case.^{17c,38} The cations **11a,b** are freely soluble in THF, and addition of a few drops of *d*₈-THF to a *d*₆-benzene solution of these complexes results in greatly simplified ¹H and ¹⁹F NMR spectra. Most significantly, three sharp ¹⁹F resonances are now observed with a Δδ_{m,p} value of 2.7 ppm (free B(C₆F₅)₃, Δδ_{m,p} = 2.6 ppm) for both compounds. A broad resonance in the ¹H NMR spectra is observed at 3.4 ppm due to the ¹¹B broadened CH₂ of the anion benzyl group. Taken together, these observations suggest that benzyl abstraction by B(C₆F₅)₃ occurs to generate an associated cation–anion pair in benzene and that THF displaces the anion to form a solvated cationic alkyl.

The ethylene polymerization activity of cations derived from **2b,d** and **7** was investigated. In all three cases, no significant polyethylene formation was observed using 1 equiv of B(C₆F₅)₃ as cocatalyst at 50 °C. However, using a large excess of methylaluminoxane (MAO, 1000 equiv) resulted in moderate polymerization activity (Table 4). This difference in reactivity may be

(35) (a) Vollhardt, K. P. C. *Angew. Chem., Int. Ed. Engl.* **1984**, *23*, 539. (b) Vollhardt, K. P. C. *Acc. Chem. Res.* **1977**, *10*, 1. (c) McAllister, D. R.; Bercaw, J. E.; Bergman, R. G. *J. Am. Chem. Soc.* **1977**, *99*, 1666. (d) Bianchini, C.; Caulton, K. G.; Chardon, C.; Eisenstein, O.; Folting, K.; Johnson, T. J.; Meli, A.; Peruzzini, M.; Rauscher, D. J.; Streib, W. E.; Vizza, F. *J. Am. Chem. Soc.* **1991**, *113*, 5127. (e) Shore, N. *Chem. Rev.* **1988**, *88*, 1081. (f) Winter, M. J. In *The Chemistry of the Metal–Carbon Bond. Carbon–Carbon Bond Formation Using Organometallic Compounds*; Hartley, F. R., Patai, S., Eds.; Wiley: Chichester, U.K., 1985; Vol. 3, Chapter 5.

(36) (a) Wielstra, Y.; Gambarotta, S.; Meetsma, A.; de Boer, J. L. *Organometallics* **1989**, *8*, 2696. (b) Calderazzo, F.; Marchetti, F.; Pampaloni, G.; Hiller, W.; Antropiusová, H.; Mach, K. *Chem. Ber.* **1989**, *122*, 2229. (c) Calderazzo, F.; Pampaloni, G.; Pallavicini, P.; Strähle, J.; Wurst, K. *Organometallics* **1991**, *10*, 896.

(37) The nature of the anion–cation interaction in **11a,b** is not known, but examples of both arylF⋯Zr and η⁶-benzyl⋯Zr binding are known. The structure depicted in eq 8 is shown with an η⁶-benzyl⋯Zr interaction for simplicity. Aryl F⋯Zr interactions: (a) Temme, B.; Karl, J.; Erker, G. *Chem. Eur. J.* **1996**, *2*, 919. (b) Horton, A. D.; Orpen, A. G. *Organometallics* **1991**, *10*, 3910. η⁶-Benzyl⋯Zr interactions: (c) Horton, A. D.; Frijns, J. H. G. *Angew. Chem., Int. Ed. Engl.* **1991**, *30*, 1152. (d) Bochmann, M.; Karger, G.; Jagger, A. J. *J. Chem. Soc., Chem Commun.* **1990**, 1038. (e) Pellecchia, C.; Immirzi, A.; Grassi, A.; Zambelli, A. *Organometallics* **1993**, *12*, 4473. (f) Horton, A. D.; de With, J. *J. Chem. Soc., Chem. Commun.* **1996**, 1375. (g) Chen, Y.; Marks, T. J. *Organometallics* **1997**, *16*, 3649.

(38) It has been suggested that a Δδ_{m,p} value of greater than 3.0 ppm is indicative of strong anion binding.^{17c}

Table 4. Ethylene Polymerization Results for Selected Group 4 Alkoxides and Related Complexes

entry	precatalyst	activity (kg mol ⁻¹ h ⁻¹)	10 ³ M _w	M _w /M _n	ref
1	2b	136			this work
2	2d	384	452	5.7	this work
3	7	68	143	3.4	this work
4	Zr[3,3'-R-1,1'-Bi-2-naph-O ₂]X ₂ ^a				5a
	R = SiMe ₃ , X = Cl	152	200	24	
	R = SiMePh ₂ , X = Cl	203	360	15	
	R = SiPh ₃ , X = Cl	275			
	R = SiPh ₃ , X = CH ₂ Ph	inactive			
5	Zr[3- <i>t</i> -Bu-5-Me-2-O-C ₆ H ₂ (CHO)] ₂ Cl ₂ ^b	8320	633	17.1	39a
	Zr[3- <i>t</i> -Bu-5-Me-2-O-C ₆ H ₂ (CHO)]Cl ₃ (THF) ^b	4400	906	16.7	
6	Ti(n-BuCp)(2,6- <i>t</i> -Bu ₂ -C ₆ H ₃ O)Cl ₂ ^c	1240	138	4.7	39b
7	ZrCp ₂ [2,6- <i>t</i> -Bu ₂ -C ₆ H ₃ O]Cl ₂ ^d	9700	225	2.7	39c
8	Zr(salen)Cl ₂ (THF) ^e	3350	77	2.5	39f
9	Zr(MeBr ₂ Ox) ₂ (CH ₂ Ph) ^f	66			39g
	Zr(MeBr ₂ Ox) ₂ (CH ₂ Ph) ^g	73	21	16.3	
	Zr(MeBr ₂ Ox) ₂ Cl ₂ ^h	15	460		
10	Zr[PyC(CF ₃) ₂ O] ₂ [CH ₂ Ph] ₂ ⁱ	96	16	2.6	39h
	Zr[PyC(CF ₃) ₂ O] ₂ [CH ₂ Ph] ₂ ^j	10	375	28	
11	Zr[pyC(4- <i>t</i> -Bu-C ₆ H ₄) ₂ O] ₂ [NMe ₂] ₂ ^k	280	88	8.3	39i
	Zr[pyC(4-NEt ₂ -C ₆ H ₄) ₂ O] ₂ [NMe ₂] ₂ ^k	120			

^a Conditions: toluene, 20 °C, 3 atm of ethylene, 500 equiv of MAO cocatalyst. ^b Conditions: toluene, 80 °C, 10 atm, 1000 equiv of MAO.

^c Conditions: toluene, 60 °C, 4 atm, 2000 equiv of MAO. ^d Conditions: toluene, 80 °C, 10 atm, 6000 equiv of MAO. ^e Conditions: toluene (suspension), 80 °C, 5 atm, 3200 equiv of MAO. ^f Conditions: 1:1 toluene/chlorobenzene, 60 °C, 3 atm, HNMePh₂⁺[B(C₆F₅)₄]⁻ cocatalyst.

^g Conditions: 1:1 toluene/chlorobenzene, 30 °C, 8 atm, HNMePh₂⁺[B(C₆F₅)₄]⁻ cocatalyst. ^h Conditions: 1:1 toluene/chlorobenzene, 30 °C, 8 atm, 680 equiv of MAO. Me₂Br₂Ox = 2-Me-5,7-Br₂-8-quinolinolato. ⁱ Conditions: benzene, 40 °C, 3 atm, 1 equiv of B(C₆F₅)₃ cocatalyst.

^j Conditions: toluene, 30 °C, 8 atm, 1000 equiv of MAO. ^k Conditions: toluene, 43 °C, 1 atm, 4:7 AlPri₃/MAO cocatalysts with an overall Al/Zr ratio of 2000:1.

attributable to strong anion coordination with B(C₆F₅)₃ as cocatalyst. The activity of catalysts derived from all three complexes is at least 1 order of magnitude lower than that of traditional zirconocene-based catalysts,^{19b,39c} the zirconocene alkoxide chloride complex studied by Repo et al. (entry 7, Table 4),^{39c} or the related salicylaldehyde^{39a} and salen^{39f} complexes (entries 5 and 8, respectively, Table 4). However, the molecular weights were relatively high and the polydispersity of the polymer was among the narrowest obtained using alkoxide-based catalysts (Table 4).^{5a,39} Interestingly, the catalyst derived from **2d** showed a distinct induction period of approximately 30 min but the highest activity once polymerization began. Since **2d** is also the only one of the three complexes which is known to be fluxional at room temperature and to participate in ligand redistribution reactions, it is tempting to attribute these observations to a slow reorganization of the metal coordination sphere to generate a more active species, possibly involving methyl–benzyl exchange with MAO.⁴⁰ The reason for the lower activity of the catalyst derived from metallacycle **7** is not clear, because the identity of the active catalyst is not immediately obvious.

(39) (a) Matilainen, L.; Klinga, M.; Leskelä, M. *J. Chem. Soc., Dalton Trans.* **1996**, 219. (b) Nomura, K.; Naga, N.; Miki, M.; Yanagi, K.; Imai, A. *Organometallics* **1998**, *17*, 2152. (c) Repo, T.; Jany, G.; Salo, M.; Polamo, M.; Leskelä, M. *J. Organomet. Chem.* **1997**, *541*, 363. (d) Sernetz, F. G.; Mülhaupt, R.; Fokken, S.; Okuda, J. *Macromolecules* **1997**, *30*, 1562. (e) Froese, R. D. J.; Musaev, D. G.; Matsubara, T.; Morokuma, K. *J. Am. Chem. Soc.* **1997**, *119*, 7190. (f) Repo, T.; Klinga, M.; Pietikäinen, P.; Leskelä, M.; Uusitalo, A.; Pakkanen, T.; Hakala, K.; Aaltonen, P.; Löfgren, B. *Macromolecules* **1997**, *30*, 171. (g) Bei, X.; Swenson, D. C.; Jordan, R. F. *Organometallics* **1997**, *16*, 3282. (h) Tsukahara, T.; Swenson, D. C.; Jordan, R. F. *Organometallics* **1997**, *16*, 3303. (i) Kim, I.; Nishihara, Y.; Jordan, R. F.; Rogers, R. D.; Rheingold, A. L.; Yap, G. P. A. *Organometallics* **1997**, *16*, 3314.

Conclusion

The aminodiolate ligands discussed here allow the successful isolation of monomeric zirconium dialkyl complexes. Notably, the fluxional behavior and thermal stability depend critically on the nature of the substituent at nitrogen. In particular, large substituents at nitrogen destabilize the compound thermally and lead to fluxional behavior in solution. While this can lead to interesting complexes such as the chiral metallacycle **7**, it is generally undesirable. In addition, the presence of an additional amine donor probably decreases polymerization activity of the alkyl cations formed with MAO by decreasing the metal Lewis acidity. Current ligand design focuses on decreasing the strength and number of donors available to the metal center with the hope of increasing the metal Lewis acidity and reactivity.

Acknowledgment. The support of the Natural Sciences and Engineering Research Council of Canada is gratefully acknowledged.

Supporting Information Available: Tables of atomic coordinates, bond distances and angles, and anisotropic thermal parameters for **7** and **8b**. This material is available free of charge via the Internet at <http://pubs.acs.org>.

OM9907324

(40) No evidence for loss of the aminodiolate ligand from zirconium in the presence of MAO (1 equiv) was observed by ¹H NMR. It would obviously be difficult to determine whether ligand loss is occurring in the presence of a very large excess of MAO; therefore, we cannot state unequivocally that this is not occurring under the polymerization conditions.